ELSEVIER

Palaeogeography, Palaeoclimatology, Palaeoecology 198 (2003) 187–221

PALAEO

www.elsevier.com/locate/palaeo

Contourite deposits in the central Scotia Sea: the importance of the Antarctic Circumpolar Current and the Weddell Gyre flows

Andrés Maldonado [a,*], Antonio Barnolas [b], Fernando Bohoyo [a], Jesús Galindo-Zaldívar [c], Javier Hernández-Molina [d], Francisco Lobo [e], José Rodríguez-Fernández [a], Luis Somoza [b], Juán Tomás Vázquez [f]

[a] *Instituto Andaluz Ciencias de la Tierra, CSIC/Universidad Granada, Facultad de Ciencias, 18002 Granada, Spain*
[b] *Instituto Geológico y Minero de España, Ríos Rosas, 23, 28003 Madrid, Spain*
[c] *Departamento de Geodinámica, Universidad de Granada, 18071 Granada, Spain*
[d] *Facultad de Ciencias del Mar, Departamento de Geociencias Marinas, Universidad de Vigo, 36200 Vigo, Spain*
[e] *CIACOMAR/Universidade do Algarve, Avenida 16 de Junho s/n, 8700-311 Olhao, Portugal*
[f] *Facultad de Ciencias del Mar, Universidad de Cádiz, 11510 Puerto Real, Cádiz, Spain*

Received 23 January 2002; accepted 3 March 2003

Abstract

New swath bathymetry with multichannel and high resolution seismic profiles shows a variety of contourite drift, sediment wave morphologies, and seismic facies in the central Scotia Sea. The deposits are to be found at the confluence between the two most important bottom current flows in the southern ocean: the eastward flowing Antarctic Circumpolar Current (ACC) and the northward outflow of the Weddell Sea Deep Water (WSDW). The contourite drifts are wedge-like deposits up to 1 km thick, that exhibit aggradational reflectors along axis thinning towards the margins. The contourite drifts occur in areas of weaker flows along the margins of contourite channels and in areas protected by obstacles. The elongate-mounded drifts are best developed along the left-hand margins of channelized bottom current flows, due to the Coriolis force. A contourite fan has a main channel and two distributary channels that expand over a gentle seafloor. The proximal fan exhibits sediment waves with the distal fan incised by furrows. Sediment wave fields are well developed in areas of intensified bottom flows without channels, particularly at the confluence of the ACC and the WSDW. Small sediment waves occur where unidirectional bottom current flows predominate. Sediment waves may develop under the influence of internal waves produced by the interaction of the flows and sea-bottom relief. The stratigraphic sequence above the oceanic crust of Early to Middle Miocene age contains six seismic units separated by major reflectors. All the units were shaped under the influence of strong bottom current flows, although they exhibit distinct seismic facies changes that record the variations of the bottom current pathways over time. The age of the units was calculated based on the age of the oceanic crust and sedimentation rates of deep-sea deposits in the region. The oldest, Units VI–IV, are of Early to Middle Miocene age and developed under the influence of the ACC. They are characterized by a southward progradational pattern of the seismic units and sedimentation rates of 5–8 cm/ky. Unit III, with an estimated Middle Miocene age, evidences the

* Corresponding author. Tel.: +34-958-244159; Fax: +34-958-271873.
E-mail address: amaldona@ugr.es (A. Maldonado).

0031-0182/03/$ – see front matter
doi:10.1016/S0031-0182(03)00401-2

first incursion of WSDW into the central Scotia Sea, when plate movement caused openings in the South Scotia Ridge and allowed the connection with the northern Weddell Sea through Jane Basin and gaps in the ridge. Unit II, estimated to be of Late Miocene to Early Pliocene age, extends over the area and is characterized by internal unconformities. A major unconformity at the base of Unit II records an important reorganization of bottom current flows that may predate the onset of grounded ice sheets on the Antarctic Peninsula shelf. Unit I, of Late Pliocene to Quaternary age, shows intensified bottom currents. The unconformity at the base of Unit I probably predates the onset of major Northern Hemisphere glaciations and the greater expansion of Antarctic ice sheets during the Late Pliocene. The extensive distribution of contourite deposits above the oceanic crust testifies to the long-term production of Antarctic Bottom Water. Cold, deep water was swept northward from the Weddell Gyre, interacting with the ACC, and possibly exerting profound influences on the global circulation system and the onset of major glaciations.

Keywords: Contourite deposits; Scotia Sea; Antarctic paleoceanography; Antarctic Circumpolar Current; Weddell Sea Deep Water

1. Introduction

The Scotia Sea developed coeval with the opening of Drake Passage, which began during the Late Paleogene (Lawver et al., 1992; Livermore et al., 1994). The opening of the new seaway between the two southern continents isolated Antarctica and allowed the initiation of the Antarctic Circumpolar Current (ACC). The thermal isolation developed by the ACC probably had a major impact on the evolution of the Antarctic ice sheets and global ocean circulation patterns (Barker and Burrell, 1977; Kennett, 1977; Lawver et al., 1992; Barrett, 1996). This current provides the only linkage between the three main Atlantic, Pacific and Indian ocean basins and facilitates the transport of heat, salt and nutrients around the globe. In addition, the production of Antarctic Bottom Water (AABW) and its influence on ocean circulation through the northward flow of deep water are well recognized (Nowlin and Klinck, 1986; Duplessy et al., 1988). The importance of the ACC and AABW on marine sedimentation and the glacial cycles has been illustrated in several studies (Pudsey et al., 1987; Rack, 1993; Diester Haass and Zahn, 1996).

During the SCAN 2001 cruise, a sector of the central and southern Scotia Sea, north of the South Orkney Microcontinent was investigated in order to analyze the bottom morphology and seismic stratigraphy of the depositional bodies (Fig. 1). An area mapped with swath bathymetry is located at the exit of a major morphologic gap in the South Scotia Ridge, north of the entrance to the Jane Basin (Fig. 2). The bathymetry ranges between 2500 m in the SE corner to more than 3500 m in the northern sector. The relief is very irregular with wide valleys, incised channels, depressions and areas of very irregular topography (Figs. 1 and 2).

We describe extensive contourite drifts and sediment wave fields that developed as a result of the interference between bottom current flows. These deposits record intense bottom current activity over time. It is shown that the opening of seaways around Antarctica not only favored the development of a strong circumpolar flow, but also induced a high production of AABW, which subsequently swept northward into the South Atlantic. We finally discuss the paleoceanographic implications of evolving seaways in the Scotia Sea since the Early Miocene and the subsequent impact of AABW flows for the onset and evolution of major glaciations.

2. Geological and oceanographic setting

The Scotia Sea is a relatively small ocean basin (1.3×10^6 km^2), that resulted from the final stages of the continental fragmentation of Gondwana and the consequent Late Paleogene separation of the Antarctic Peninsula from South America (Barker et al., 1991; Livermore et al., 1994). The Drake Passage developed following the dispersal of the continental blocks that formed the

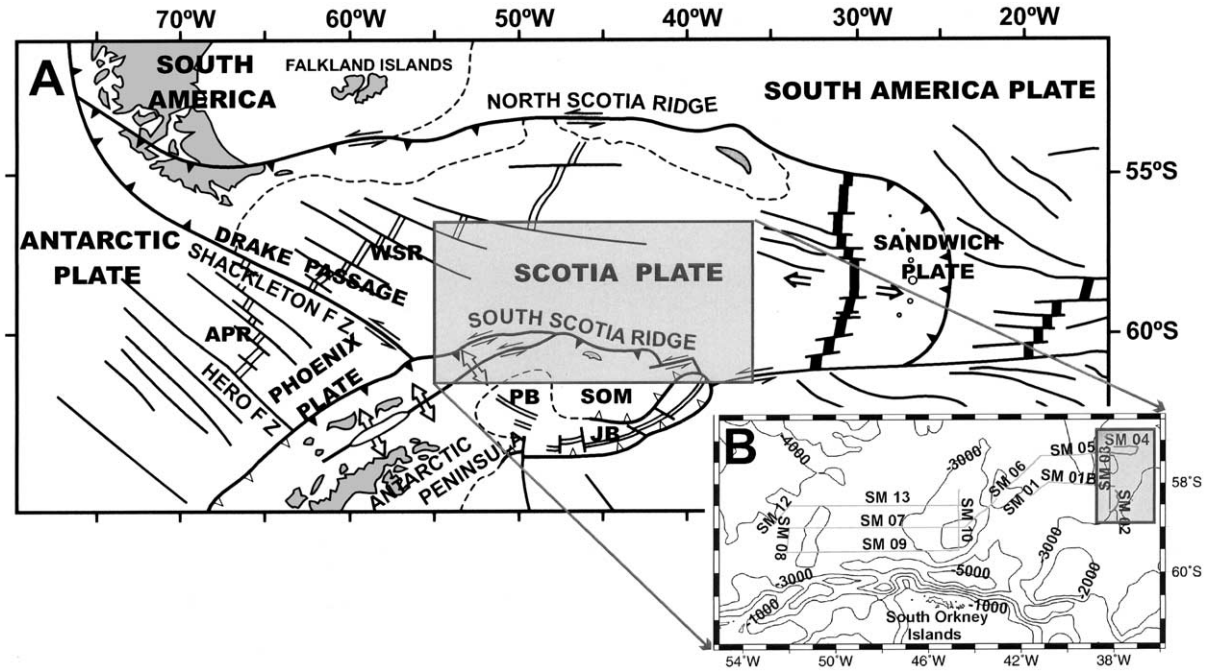

Fig. 1. (A) Geological setting of the Scotia Sea; the rectangle indicates the study area. (B) Bathymetry of the study area and location of the SCAN 2001 profiles and swath bathymetry area (shaded). Water depth in meters.

bridge between the two southern continents (Lawver et al., 1992). The Scotia Sea is shaped at present by two active plates confined by the Shackleton Fracture Zone to the west and the Scotia Arc on the three other sides (Fig. 1). This arc is composed of the North and South Scotia Ridge and the South Sandwich fore-arc (British Antarctic Survey, 1985; Pelayo and Wiens, 1989; Larter et al., 1998; Barker, 2001). The oldest marine magnetic anomalies of the Scotia Sea occur in the western sector, where chrons C9 and C10 are identified in the northwestern area, whereas anomaly C8 is consistently observed (British Antarctic Survey, 1985). The southwestern Scotia Sea includes, however, an area of oceanic floor about 100 km wide without magnetic anomalies between chron C8 and the continental margin. The earliest stages in the opening of the Drake Passage reveal average half spreading rates of 28 mm/yr (Maldonado et al., 2000), which applied to the area of oceanic crust without magnetic anomalies, implying an initiation of seafloor spreading before 30 Ma. The oceanic floor in the study area contains E–W oriented short magnetic anomalies with chrons C6 and C5C (20.1–16.0 Ma).

The North and South Scotia Ridge are two complex structural features formed by a mixture of continental fragments and remnant arc elements, which accommodate and transfer westward the motions between the South American and Antarctic plates (Pelayo and Wiens, 1989; Livermore et al., 1994). The ridges have a complex morphology, with basins up to 5 km deep and banks less than 1 km deep. The majority of the basin plain of the Scotia Sea is located at depths of 3000–4500 m, and it is isolated from major sources of sediment supply at the continental margins (Fig. 1). Only the western sectors of this sea have direct access to sediment sources from South America and the northern tip of the Antarctic Peninsula. The study area is fully cut off from direct sediment supply, since it is isolated from the nearby South Orkney Microcontinent by a deep depression between the microcontinent and two prominent submarine banks to the south (Fig. 2).

The present circulation in the Scotia Sea has

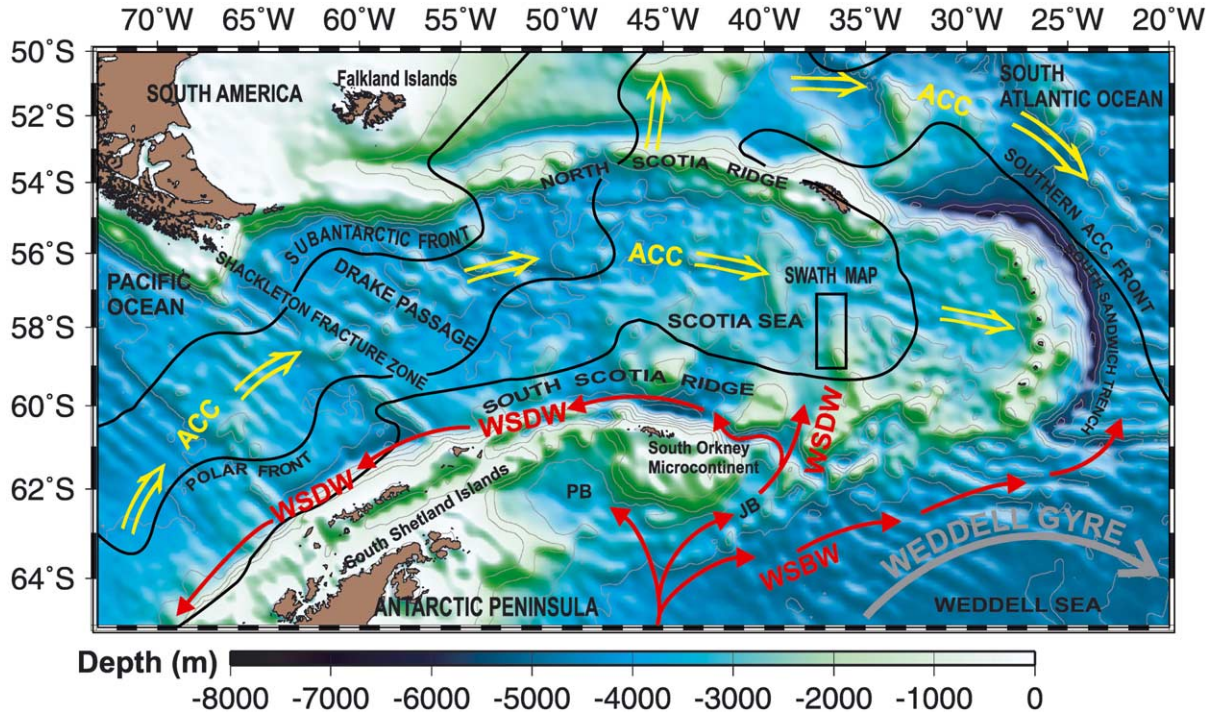

Fig. 2. Main bathymetric and oceanographic features of the Scotia Arc region. Open arrows indicate the Antarctic Circumpolar Current (ACC). Solid arrows show Weddell Sea Bottom Water (WSBW) and Weddell Sea Deep Water (WSDW) associated with the Weddell Gyre. The Subantarctic, Polar and Southern ACC density gradient fronts connected with the eastward flow of the ACC are shown. Abbreviations: PB, Powell Basin; JB, Jane Basin.

two main components: (1) in the north, the ACC flows eastward, and (2) in the south, the Weddell Sea Deep Water (WSDW) flow moves northward from the Weddell Gyre (Fig. 2). Bottom potential temperatures are warmer near the North Scotia Ridge (+0.2°C) and cooler in the proximity of the South Orkney Islands (−0.6°C), reflecting a bottom water origin of the ACC in the north and one of the WSDW in the south Scotia Sea (Locarnini et al., 1993; Orsi et al., 1995). The ACC is forced by westerly winds from the SE Pacific into the Scotia Sea, mostly across the northern part of Drake Passage (Nowlin and Zenk, 1988; Orsi et al., 1995; Moore et al., 1997). The ACC extends to the seafloor in the Scotia Sea. It is proposed that much of the flow occurs within narrow jets associated with two water mass fronts – the Polar and the Subantarc-

Fig. 3. Swath bathymetry of the study area showing the main contourite deposits and channels related to the Antarctic Circumpolar Current (ACC) and Weddell Sea Deep Water (WSDW). The North, Middle and Southern Antarctic channels (NAC, MAC and SAC) are the main channels of the ACC. A1 and A3 are elongate-mounded contourite drifts related to channelized branches of the ACC; A2 is a large sediment wave field. The Weddell channel (WC) is the main channel of the WSDW. The contourite deposits associated with the WSDW include W1–W4. W1 is a slope-plastered drift attached to the western margin of Discovery Bank. W2 is composed of an elongate-mounded drift and sediment waves. W3 is a contourite fan formed by two distributary channels. W4 is composed of a sheeted drift and sediment waves. Bottom current directions are also shown, based on contourite channels, drift depositional trends and sediment wave migration patterns. WAB is the boundary between the ACC and WSBW bottom flows. Open arrows show the ACC bottom flows and solid arrows indicate WSDW flows. The line drawing interpretation of the contourite deposits is illustrated in Fig. 5.

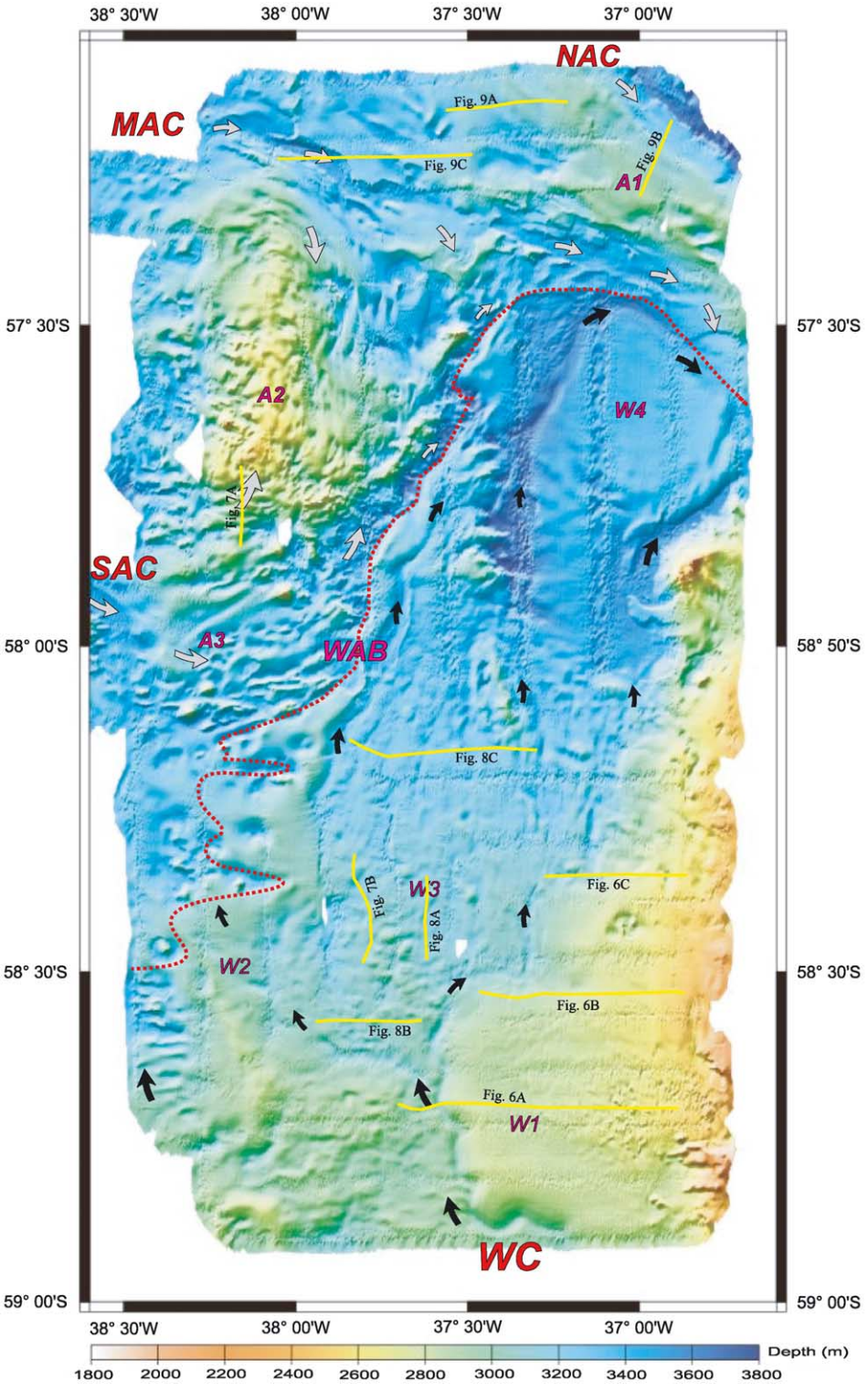
38° 30'W
38° 00'W
37° 30'W
37° 00'W
57° 30'S
58° 00'S
58° 30'S
59° 00'S
58° 50'S
NAC
MAC
SAC
WAB
WC
A1
A2
A3
W1
W2
W3
W4
Fig. 9A
Fig. 9B
Fig. 9C
Fig. 7A
Fig. 8C
Fig. 7B
Fig. 8A
Fig. 6C
Fig. 6B
Fig. 8B
Fig. 6A
Depth (m)
1800
2000
2200
2400
2600
2800
3000
3200
3400
3600
3800

tic fronts – that are bands of large horizontal density gradients continuous around Antarctica (Peterson and Whitworth, 1989; Gille, 1994). The ACC splits within the Scotia Sea into an eastward component and a northeastward component, which flow into the Southwest Atlantic through morphologic gaps (Fig. 2). For example, an important seaway in the North Scotia Ridge for the ACC is the gap at 48°W known as the 'Shag Rocks Passage', where average speeds of 17 cm/s to the WNW have been reported (Zenk, 1981; Howe and Pudsey, 1999)

The majority of the WSDW in the Scotia Sea is derived from the Weddell Sea Bottom Water (WSBW). The WSBW flows clockwise in the Weddell Sea, following the Weddell Gyre southward of the ACC (Fahrbach et al., 1994; Schröder and Fahrbach, 1999). The WSBW escapes northward at about 3000 m water depth from the northwestern Weddell Sea to the Scotia Sea through deep gaps in the South Scotia Ridge and contributes to the WSDW (Fig. 2). The flow is channelized along the Powell and Jane Basins (Foster and Middleton, 1979, 1980; Pudsey et al., 1987; Howe et al., 1998). The WSBW also flows northward along the South Sandwich Trench towards the South Atlantic, where it joins the WSDW exiting the Scotia Sea across gaps of the North Scotia Ridge (Georgi, 1981; Locarnini et al., 1993). Some WSDW also escapes the Scotia Sea westwards along the South Scotia Ridge and then flows towards the Pacific margin of West Antarctica (Camerlenghi et al., 1997). Probably up to 80% of the AABW is formed in the Weddell Sea, whereas the deep WSBW constitutes the densest variety of AABW (Foldvik and Gammelrsød, 1988). Bottom water with an Antarctic source flows north through the western Atlantic as far as 35°N and is modified by mixing with overlying water masses. The Scotia Arc is a morphologic barrier to the path of these flows (Pudsey, 1992; Howe et al., 1998; Pudsey and Howe, 1998).

3. Methods

During the 2000–2001 austral summer season, an area of the central and southern Scotia Sea, north of the South Orkney Microcontinent, was investigated with the Spanish vessel B/O *Hespérides* (Fig. 1B). A total of 2072 km of multichannel seismic (MCS) profiles was obtained along 11 tracklines, collected together with high resolution seismic profiles, swath bathymetry, and magnetic and gravity measurements. An area of about 200×100 km^2 was also mapped with swath bathymetry and, in addition, high resolution profiles as well as magnetic and gravity measurements were taken along these swath ship tracks. Five of the MCS profiles are located within the swath area.

The multichannel reflection seismic profiles were obtained with a tuned array of 5 BOLT air guns with a total volume of 22.14 l and a 96-channel streamer with a length of 2.4 km. The shot interval was 50 m and the data were recorded using a GEOMETRIC Strata Visor™ digital system at a sampling record of 2-ms interval and 12-s length. The data were processed with a standard sequence, including migration using a DISCO/FOCUS system. High resolution subbottom profiles were obtained with a Topographic Parametric Source (TOPAS) BENTECH Subsea PS018 operated at 1.5–4.0 kHz and digitally processed in real time.

The swath data were obtained with a SIMRAD EM 12 system and post-processed with the NEPTUNE software and FLEDERMAUS for visualization. Total intensity magnetic field data were recorded with a Geometrics G-876 proton precession magnetometer along the ship tracklines. Data were acquired every 5 s. The processing includes elimination of spikes and filtering using a running mean to obtain one value every 2 min. The magnetic anomalies were calculated using the IGRF 2000 (IAGA, 2000). Gravity data were acquired with a Bell Aerospace TEXTRON BGM-3 marine gravimeter.

4. Depositional bodies and erosional features influenced by the ACC and WSDW

The swath bathymetry map shows an irregular bottom relief and a variety of depositional and

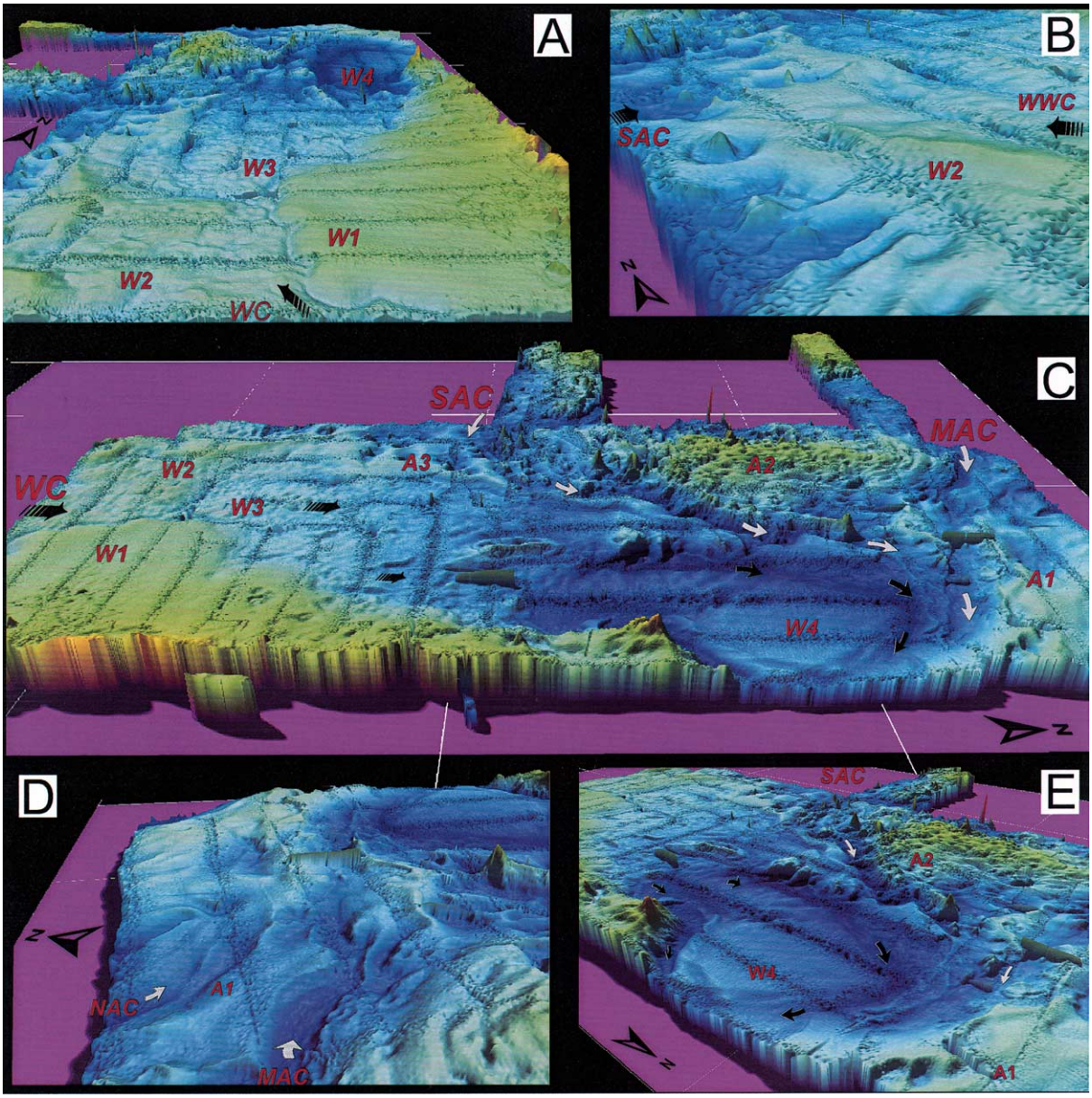

Fig. 4. 3-D imagery from multibeam bathymetry showing the main contourite deposits and channels of the study area. Nomenclature is the same as in Fig. 3. (A) South-to-north view of the sedimentary fields associated with the WSBW current. Two large drift deposits (W1 and W2) are formed at both sides of the main channel of the WSDW. The Discovery Bank appears as prominent relief on the right. Note the fan-like shape and the distributary channels of the contourite fan system (W3). (B) Detailed view of the westernmost boundary of the WSBW flow that forms an elongated drift and large sediment waves fields (W2). (C) South-to-north view of the overall study area showing the relationship between the WSBW and ACC. Note that the ACC current is bifucarted into two branches (SAC and MAC) as a consequence of the basement relief giving rise to climbing large sediment waves fields (A2). (D) Detailed view of the northernmost channels of the ACC current (NAC and MAC), forming a large elongate-mounded drift (A1). (E) Detailed view of a complex contourite deposit (W4) and the interaction between the ACC and WSBW flows. Deposit W4 made up of a mounded-sheeted drift and large asymmetric waves apparently formed by the clockwise gyre of the WSDW and its interaction with the ACC current.

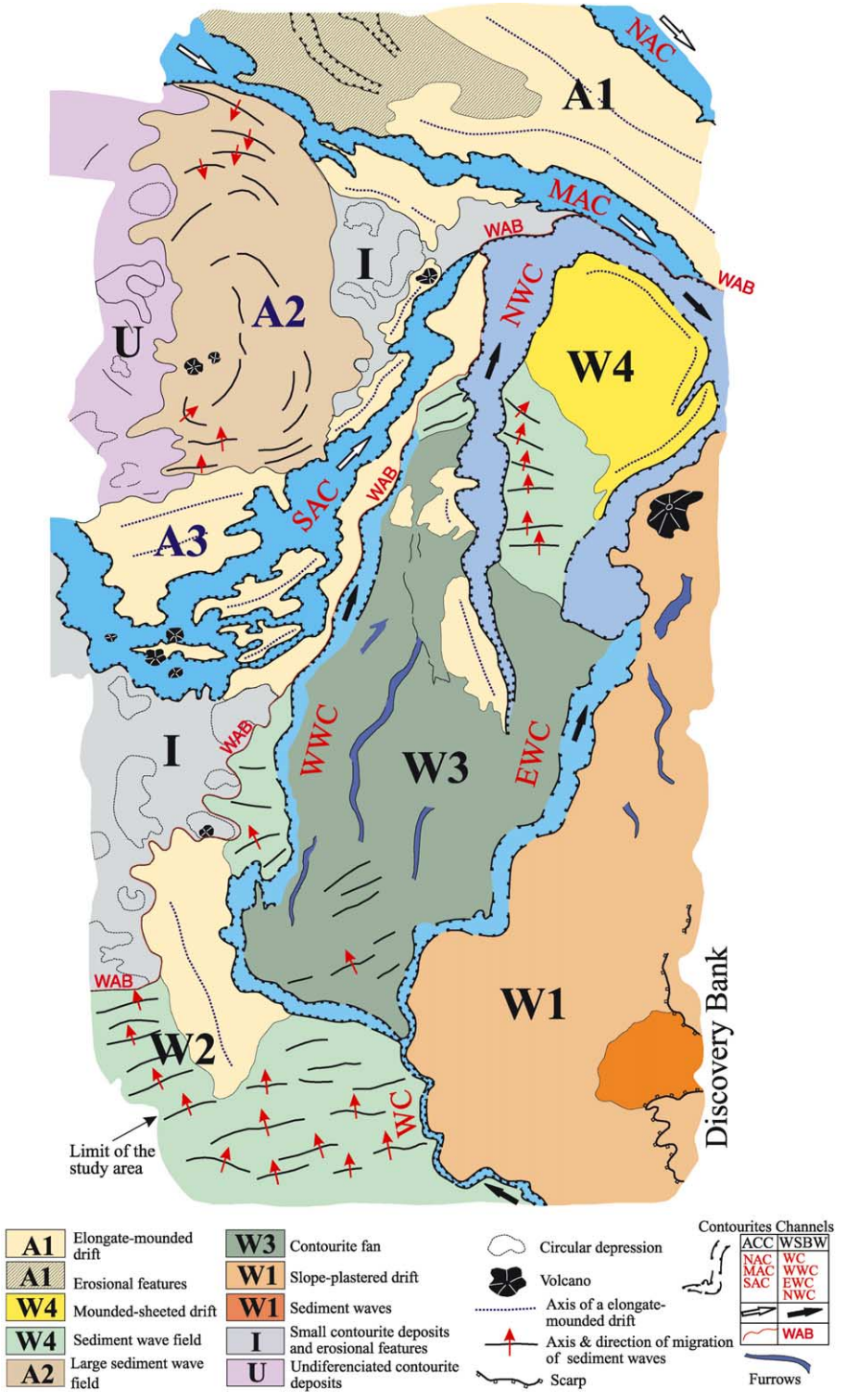
NAC
A1
MAC
WAB
I
A2
U
NWC
W4
WAB
SAC
WAB
A3
I
WAB
WWC
W3
EWC
W1
WAB
W2
WC
Limit of the study area
Discovery Bank
A1 Elongate-mounded drift
A1 Erosional features
W4 Mounded-sheeted drift
W4 Sediment wave field
A2 Large sediment wave field
W3 Contourite fan
W1 Slope-plastered drift
W1 Sediment waves
I Small contourite deposits and erosional features
U Undiferenciated contourite deposits
Circular depression
Volcano
Axis of a elongate-mounded drift
Axis & direction of migration of sediment waves
Scarp
Contourites Channels
ACC WSBW
NAC WC
MAC WWC
SAC EWC
NWC
WAB
Furrows

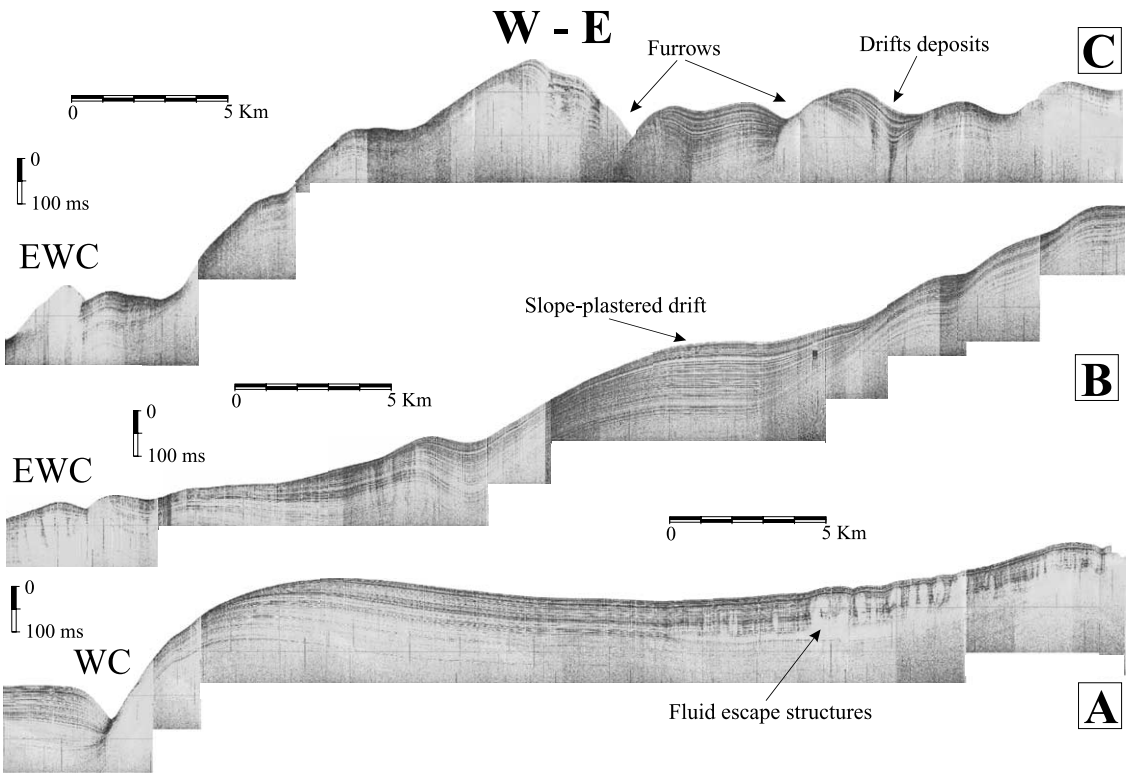

Fig. 6. Selected segments of high resolution Topographic Parametric Source (TOPAS) profiles showing three examples of the slope plastered drift (W1). The profiles are W–E oriented and arranged from south (below) to north (above). (A) Seismic profile with fluid-escape structures evidenced by a mushroom-like geometry and undulating facies in the southern sector, close to the Discovery Bank. (B) Typical seismic facies of the slope-plastered drift. (C) Furrows and drifts of the northern sector. Location of profiles in Fig. 3.

erosional morphologies (Figs. 3–5). The seismic profiles exhibit, moreover, a very irregular distribution of the depositional sequences. The deposits vary between over 1 s (twt) thick at the axis, to marginal areas where erosion and non-deposition are observed (Figs. 6–10). The morphological and seismic characteristics of the thickest units are indicative of deposits developed by processes related to bottom contour currents. The features include: (1) major discontinuities that can be traced across the area, (2) lenticular convex-upward geometries, and (3) progradational and aggradational reflectors that converge towards the marginal zones of the depositional bodies and are truncated by nu-

Fig. 5. Line drawing interpretation of the swath bathymetry map, complemented with the analysis of the seismic profiles, showing the main depositional and morphological features of the area. Legend: North, Middle and Southern Antarctic channels (NAC, MAC and SAC) are the main channels of the ACC. A1 and A3 are elongate-mounded drifts related to channelized branches of the ACC; A2 is a field of large sediment waves. The Weddell channel (WC) is the main channel of the WSBW. The Western, Eastern and Northern Weddell channels (WWC, EWC and NWC) are the main channels of the WSDW. W1 is a slope-plastered drift attached to the Discovery Bank. W2 is made up of elongate-mounded drift and sediment waves related to the WSDW. W3 is a contourite fan formed by two channels. W4 is composed by mounded-sheeted drift and sediment waves related to the WSDW. Bottom current directions are also shown based on the drift depositional patterns, channel orientation and direction of migration of sediment waves. WAB is the boundary between the ACC and the WSBW flows. See Figs. 3 and 4 for the swath map and 3-D views of the area.

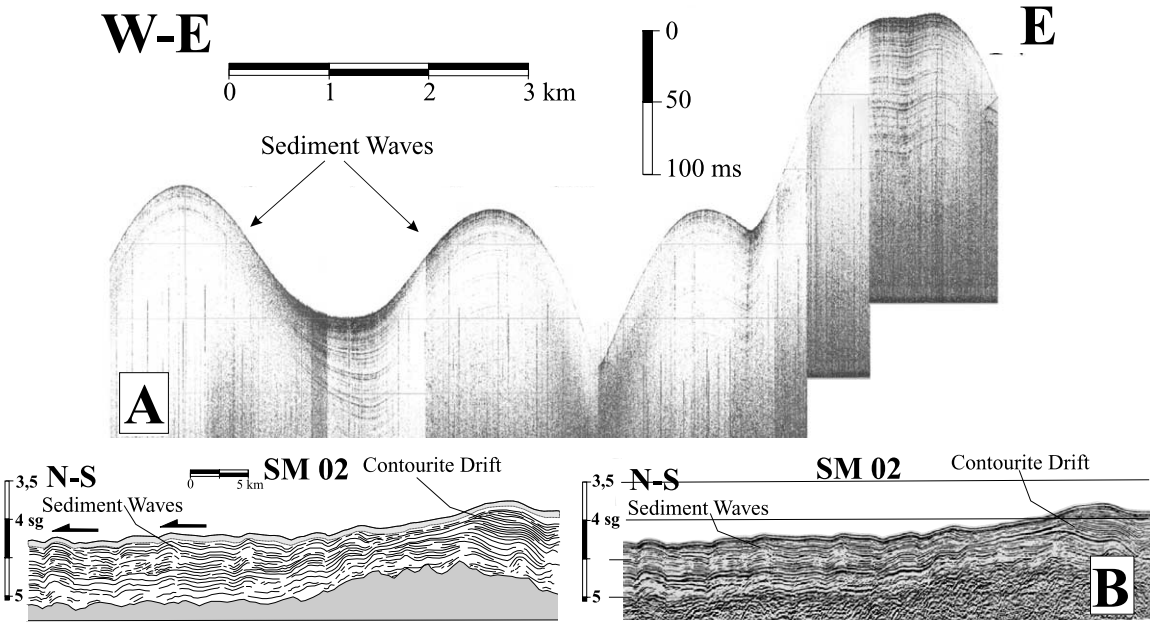

Fig. 7. Selected segments of seismic profiles showing examples of contourite sediment waves. (A) TOPAS profile segment showing sediment waves. (B) MCS profile and line drawing interpretation to illustrate the elongate-mounded drift and sediment wave field associated with the complex contourite deposit W2. Location of profiles in Fig. 3.

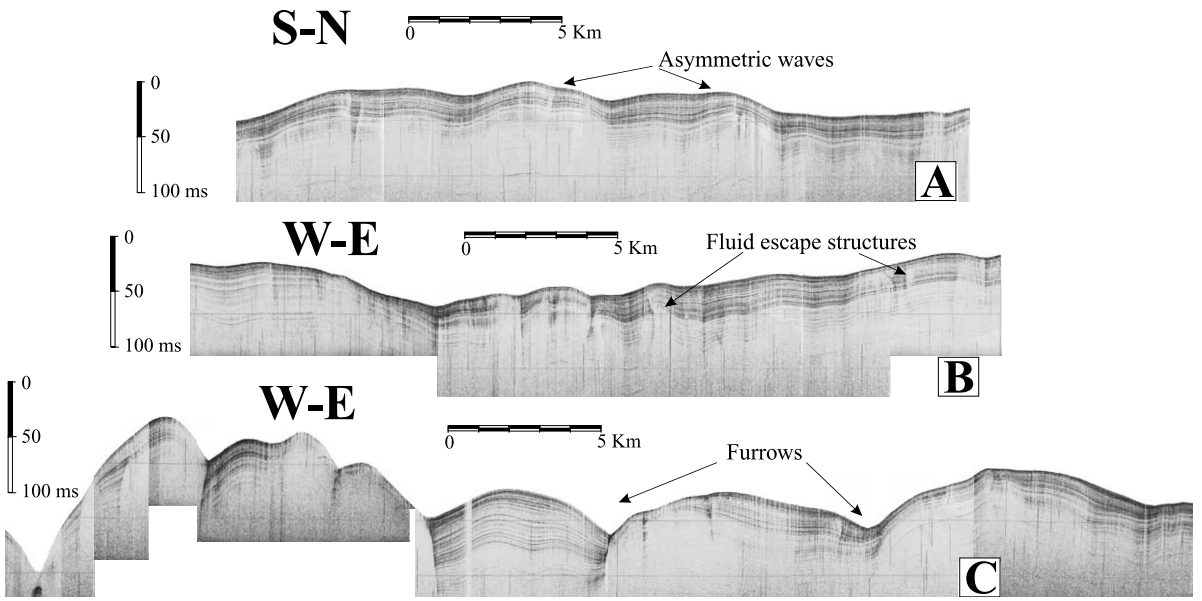

Fig. 8. Representative TOPAS profiles of the contourite fan (W3), arranged from south to north. (A) Proximal sector of the fan with a smooth and flat morphology showing an extensive asymmetric wave field. (B) Middle fan sector showing fluid escape structures. (C) Northern sector characterized by several incised furrows. Location of profiles in Fig. 3.

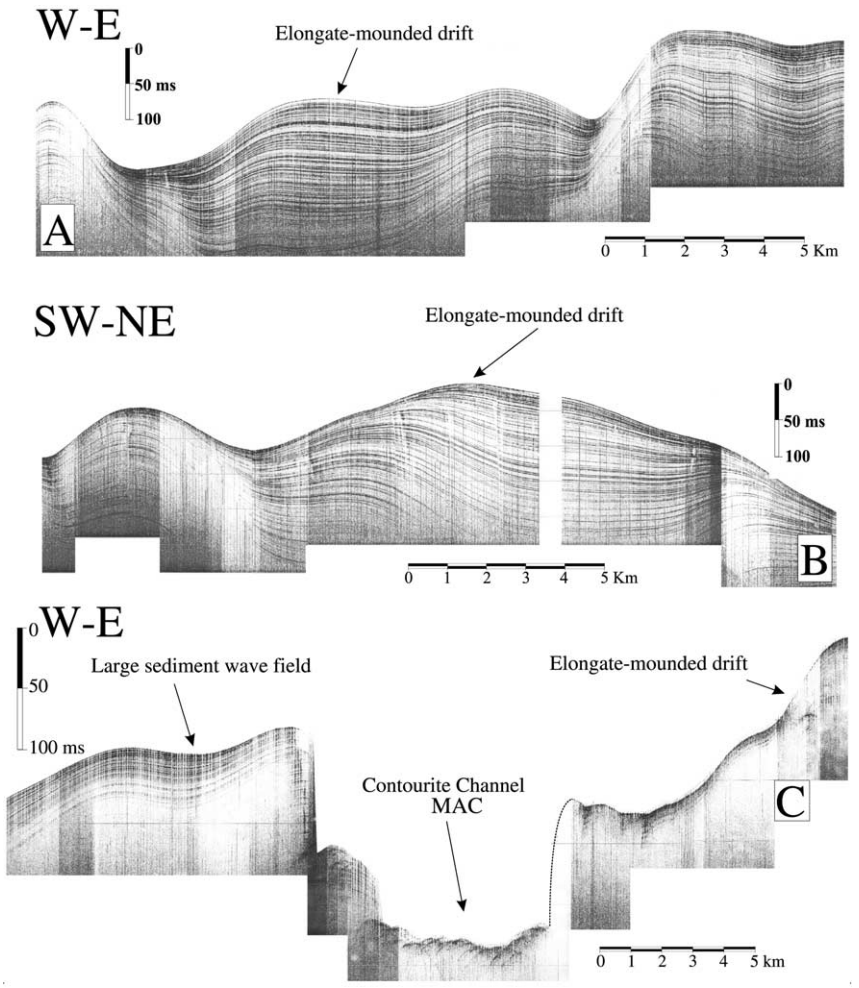

Fig. 9. Selected TOPAS profile segments showing examples of contourite deposit and channel. (A,B) Elongate-mounded drift A1. (C) Contourite Middle Antarctic Channel (MAC) representing one of the main channels of the ACC. Note the steep flanks and also the hyperbolic echo-character on the bottom of the channel. Location of profiles in Fig. 3.

merous internal discontinuities. These deposits are classified in this paper according to the nomenclature for contourite drifts, proposed by McCave and Tucholke (1986) and more recently by Faugeres et al. (1999).

Swath bathymetry and seismic profiles also show well developed sediment wave fields. Sediment waves are observed in isolated fields of deposits, or associated with and superimposed upon the contourite drifts. Complex deposits formed by the combination of several of these types were also identified. We use the general term 'contourite deposits' for all the above types of depositional bodies developed by bottom contour current processes. The deposits of the southern sector of the study area show a predominantly northward trend, whereas in the northern sector they mostly have an east–southeastward orientation (Fig. 3). As discussed below, all these deposits appear to be directly related to the nature and distribution of the bottom currents that are active in the Scotia Sea; i.e. (1) the WSDW as a component of the WSBW, with a predominantly northward trend, and (2) the ACC, with an east–southeastward trend. These flows interact with Coriolis force (Figs. 2 and 3). The contourite deposits – de-

Table 1
Main nomenclature and characteristics of the different contourite deposits related to the ACC and WSBW flows

Contourite deposits				
Nomenclature	Type	Orientation	Morphology	Seismic Facies
Related to WSDW				
W1	Slope-plastered drift	N–S	Sheeted and channel	Sub-parallel, high-amplitude reflectors. Wavy facies, fluid-escape features, transparent wedge
W2	Elongate mounded drift	NNW–SSE	Mounded, asymmetric profile	Stratified, highly aggradational
	Sediment wave fields	ENE–WSW (wave crests)	Undulating pattern	Stratified, moderate to low amplitude wavy reflectors
W3	Contourite fan	N–S	Sheeted (smooth, flat upper surface); occasional development of sediment waves	Stratified, highly aggradational. Wavy facies
W4	Mounded-sheeted drift	Not identified (probably radial)	Sheeted, linguoid. Asymmetric profile	Stratified, highly aggradational
	Sediment wave field	E–W and NW–SE (Wave crests)	Undulating pattern	Wavy facies
Related to ACC				
A1	Elongate-mounded drift	NNW–SSE	Mounded, asymmetric profile	Progradational facies towards the flanks, aggradational in the body center
A2	Large wave fields	E–W (Wave crests)	Undulating pattern	Wavy facies
A3	Small elongated drifts	NE–SW	Undulating sea-bottom floor	Not identified

scribed in detail below – are summarized in Table 1.

4.1. Contourite deposits

4.1.1. Deposits related to the WSDW

A slope-plastered drift (W1) is located in the southeastern sector, adjacent to the western margin of Discovery Bank (Figs. 3, 4A and 5). This drift deposit is characterized by a prominent westward progradation of the internal reflectors, whereas the main axis of the body trends northwards (Fig. 6). Drift W1 expands up and downslope and is characterized by a sheet shape and an aggradational reflector configuration. The drift deposit is narrower and becomes incised by several furrows in the northern sector, where it displays several independent drifts bodies and a channelized morphology (Fig. 6C). Typical seismic facies are stratified and sub-parallel, with high and low amplitude reflectors (Fig. 6B). In specific zones close to Discovery Bank, an undulating near-surface pattern of reflectors is observed, intruded by numerous subbottom structures with a mushroom-like geometry (Fig. 6A). In the southern sector, a transparent wedge-shaped deposit of limited lateral extension develops inside the slope drift, which is attributed to a mass-gravity process initiated by the nearby bathymetric high along the relief of Discovery

Fig. 10. Foldouts with representative MCS profiles and line drawing interpretations. (A) N–S profile SMC 03 showing the distribution of the stratigraphic units and contourite deposits in the western area. (B) E–W profile SMC 04 in the northern area showing elongated-mounded drift A1, sediment waves and contourite channels associated with the ACC. (C) Profile SMC 05 in the northern area showing a complete succession of the main depositional units and reflectors identified in the area. (D) Detail of profile SMC 03 showing a southward progradational body of Unit IV and the erosional features of reflectors A and C, which represent the basal unconformities of Units I and III, respectively. See Fig. 11 for the summary of the seismic stratigraphy. Location of profiles in Figs. 2 and 3.

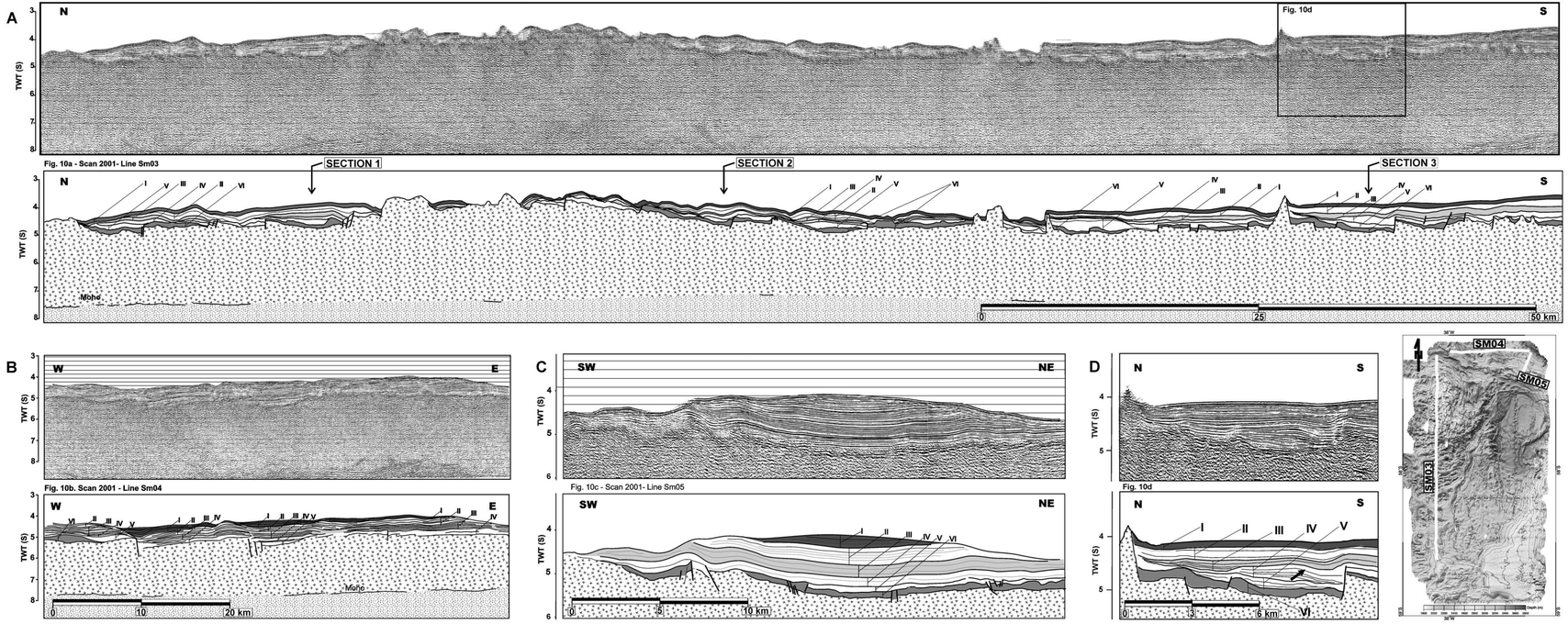
A
N
S
Fig. 10d
TWT (S)
Fig. 10a - Scan 2001- Line Sm03
SECTION 1
SECTION 2
SECTION 3
Moho
0
25
50 km
B
W
E
Fig. 10b. Scan 2001 - Line Sm04
0
10
20 km
C
SW
NE
Fig. 10c - Scan 2001- Line Sm05
0
5
10 km
D
0
3
6 km
SM04
SM05
SM03

Bank. The mushroom-like deformation structures are rooted in this wedge and they may represent fluid escape structures formed by the rising of fluidized, plastic deposits.

In the southwestern sector, a complex contourite deposit (W2) is identified at the western margin of a channel (Figs. 3, 4A and 5). Two main depositional types are differentiated in this body: (1) an elongated mounded drift, and (2) sediment wave fields. The elongated drift has a mounded, asymmetric profile, a steeper southwestern flank, and a main axis trending NNW–SSE. The shallower depth at the top of the drift is 2800 m. The seismic facies are stratified, with a strongly aggradational pattern and lateral pinching out of the reflectors towards the NE and SW (Fig. 7B). The sediment wave fields are distributed to the east and south of the elongated drift (Figs. 4B and 5). These waves are asymmetric and develop an undulating pattern on the seafloor (Fig. 7). There are two scales of sediment waves: the small waves are 2–3 km long and up to 20 m high, and the large waves range from 8 to 10 km in length and from 30 to 75 m in height. The main orientation of wave crests is ENE–WSW, but a net migration direction was not identified. Hyperbolic echoes are locally observed in association with the depressions separating adjacent sediment wave fields. Sediment waves consist of internally stratified reflectors of moderate to low amplitude and an overall low reflectivity.

A contourite fan (W3) occupies a large proportion of the central area of the swath map (Figs. 3–5). It is bounded at the eastern and western margins by two contourite channels: the Eastern (EWC) and Western Weddell Channels (WWC), which are distributaries of a main channel located up-current (WC) to the south (Figs. 3, 4A,C and 5). These two channels isolate the contourite fan from the slope-plastered drift (W1) and the contourite deposit (W2) on the eastern and western margins, respectively. The fan shows a predominantly N–S trend, with the apex located at the bifurcation of the main channel (WC) of this area. The morphology in the southern (proximal) sector of the fan is smooth and flat, showing extensive (up to 20 km), low amplitude (20–40 m), and northwards-oriented asymmetric waves (Fig. 8A). The northern (distal) fan sector is dissected by several furrows, some 60–75 m deep and 1–1.5 km wide, and associated sediment drifts (Fig. 8C). The seismic facies are stratified and highly aggradational, showing undulations several km long which mimic the seafloor morphology (Fig. 8). The undulating pattern becomes more apparent northward related to the occurrence of minor, independent contourite drift deposits associated with channels. We also find evidence of gas escape structures inside this body, especially in the southern area. In general, the deposit thins out towards the bounding channels at the margins of the fan (Fig. 8B).

A complex contourite deposit (W4) is located in the northern area, which includes two main sedimentary types (Figs. 3, 4E and 5). The first is a detached sheeted drift with an asymmetric profile and an abrupt eastern flank. The surface morphology is flat increasing in depth westwards. The shallowest water depth of the seafloor is 3200 m. In map view, the body shows a linguoid geometry. The internal seismic facies are stratified, with aggradational reflectors. The sediment thickness gradually decreases towards the margins. The second depositional type is a sediment wave field developed south of the sheeted drift (Fig. 5). Several large-scale, northward-oriented asymmetrical sediment waves (10–15 km in length, 75 m in height) are superimposed by small-scale waves (4–5 km in length, 15–25 m in height). The wave crests are oriented E–W in the south and gradually become NW–SE oriented towards the north. Internal undulating reflectors characterize these sediment waves.

4.1.2. *Deposits related to the ACC*

A detached elongated drift (A1) is located in the northeastern area of the swath map. It has a mounded morphology and asymmetric profile, with a more abrupt flank facing southwards (Figs. 3, 4D and 5). The drift is laterally constrained by two channels, the Northern and Middle Antarctic Channels (NAC, MAC; Figs. 4 and 5). The main depositional body shows a NNW–SSE orientation and is located at water depths below 2900 m. Internal progradational reflectors are observed in the northern and southern areas,

whereas the middle segment is characterized by a net aggradational stacking pattern (see Fig. 9).

A large sediment wave field (A2) is distributed over a basement high of oceanic crust in the northwestern sector, to the west of W3 (Figs. 3, 4C and 5). The axis of the depocenter has an N–S trend. Two main orientations of large waves are identified on the high (Fig. 5): (1) on the southern flank, sediment waves are 7–8 km long and 75–110 m high, and predominantly oriented northwards, and (2) on the northern flank, sediment waves are up to 15 km long and 80–110 m high with superimposed smaller waves roughly 2 km long and 20 m high, preferentially oriented southwards.

An small elongated drift (A3) is also found in the middle to northern sector of the swath map. This body has a NE–SW orientation and it is located at the southern tip of A2 (Figs. 3 and 5).

All these deposits create an undulating, irregular seafloor relief, with alternating highs and depressions. The internal character of these deposits in high resolution profiles is not well identified due to poor penetration of the acoustic signal. In MCS profiles, however, the deposits are characterized by mounded undulating reflectors and multiple internal disconformities (Fig. 10A).

4.1.3. Deposits related to the Weddell Antarctic Boundary

We designate as the zone of transition between the deposits related either to the AAC or the WSDW as the Weddell Antarctic Boundary (WAB). In this transitional zone, two areas are characterized by the occurrence of thin, irregular contourite deposits (I), whereas the rest of the region shows numerous erosional features developed by bottom currents (Figs. 3, 4C and 5). The depositional bodies are located in: (1) the central-western sector of the swath map, between W2 and A3; and (2) the northern part of the study area, between W3 and A2 (Fig. 5). The most typical erosional features are widespread circular depressions around obstacles such as submarine volcanoes and seamounts, with a vertical relief of about 100–300 m water depth and a diameter of 5–15 km in map view (Fig. 4B).

4.2. Contourite channels

4.2.1. Channels related to the WSDW

A channel (WC) located in the southern sector shows a NNW–SSE orientation for about 36 km (Figs. 3, 4A and 5). The channel floor is 0.5–2 km wide, while water depth is about 3000 m and the relief of the walls is approximately 100 m. This channel bifurcates northward into two distributary channels, the EWC and WWC. The EWC displays a NNE–SSW orientation and an estimated length of about 72 km. Channel bottom water depth increases northwards from 3000 to 3200 m. The channel floor is 2–6 km wide, increasing northwards and the walls are 100–200 m high. The WWC displays a WNW–ESE orientation for about 30 km, and then becomes oriented NNE–SSW for more than 80 km, after a meandering bend. Water depth of the WWC channel floor increases northwards, from 3000 to 3300 m. Channel width shows a similar trend to that of the EWC, becoming wider to the north (1–4 km). The western wall of the WWC is steeper than the eastern one and reaches 100 m of relief. Additionally, the eastern wall is subdued or absent in several sectors of the channel segment with the NNE–SSW orientation.

The Northern Wendell Channel (NWC) is located in the northern area of the swath map, eroded into W3 (Fig. 10). This channel is narrow in its southern part (1.5 km) and becomes very wide northwards (12 km). The channel shows a prominent N–S orientation in the southern part for most of its length, to describe an open, semicircular bend in the northern sector around W4 (Figs. 3, 4C,E and 5). Its total length is about 160 km. Water depth of the channel floor ranges between 3300 and 3700 m, with maximum depths identified in the middle part of the first N–S stretch. The walls are up to 200 m high. The channel is subdued to the northeast and displays a termination with a cirque-like morphology in map view.

4.2.2. Channels related to the ACC

Three channels observed in the northern and western areas of the swath map with predominantly WNW–ESE and NW–SE to SE–NW

arched orientations are attributed to the influence of the ACC. These channels are called the NAC, MAC and Southern Antarctic Channel (SAC). The NAC, identified at the NE corner of the swath map, bounds the northern margin of drift A1 (Figs. 3, 4C,D and 5). The MAC channel parallels the NAC and is situated across the swath area at the southern margin of drift A1 (Fig. 9C). Water depth in the smooth, flat MAC channel floor increases northwestward, from 3400 to 3500 m. Channel floors are 2–7 km wide and the walls bounding the channels have a relief of about 150–200 m. The relief between the channel floor and the crest of the bounding drift is several hundred meters of water depth. These two channels seem to be diverted from the main ACC flow around the A1 drift.

The SAC has an arched shape around contourite deposits A3, A2 and I (Fig. 5). It is formed by a wide NW–SE depression in the western part, which becomes narrower along its path and has a NE–SW oriented channel in the western and central part of the swath map (Figs. 3, 4C,E and 5). Water depth of the channel floor increases to the NE from 3300 to 3500 m and channel width is variable (3–9 km). The channel walls have several hundred meters of relief. The physiography of the channel floor is also highly irregular due to the occurrence of circular depressions.

4.3. Contourite deposits and channels: a summary of findings

Four main contourite deposits (W1–W4) are identified with a predominant south-to-north trend, having developed under the influence of the WSDW flows (Figs. 3–5; Table 1). A slope-plastered drift (W1) occurs adjacent to the western margin of Discovery Bank, whereas an elongated-complex contourite deposit (W2) occupies the southwestern sector of the swath map (Fig. 4A). These contourite drifts confine a contourite fan (W3) fed by a main channel and two distributaries (Fig. 4A,C). The northernmost body (W4) is made up of a sheeted drift deposit and large asymmetric sediment waves developed under the influence of a WSDW clockwise gyre, which is probably a consequence of the interaction of WSDW with ACC flows.

The contourite deposits related to the ACC (A1–A3) are observed in the northern and northwestern sector. One of these bodies (A1) has a characteristically WNW–ESE trend, whereas the other two bodies (A2, A3) are more complex and show an irregular sediment distribution. The elongated drifts deposits (A1, A3) are developed by bifurcating flow branches, whereas the large sedimentary wave fields (A2) result from current flows interacting with basement irregularities (Figs. 3 and 4C–E; Table 1). The zone of transition between the contourite deposits developed by the AAC or the WSDW, that is the WAB, shows two elongated areas with contourite deposits (I) and numerous erosional features (Figs. 3 and 4B).

In addition to the depositional bodies, several large erosional features such as channels and distributaries (WC, WWC, EWC, NWC, SAC, MAC, NAC) occur in the swath map area associated with bottom current flow pathways (Figs. 3 and 5).

5. Seismic stratigraphy

The MCS profiles show a sequence of depositional units above the basement represented by Layer 2 of the oceanic crust (Fig. 10). The basement, characterized by high-amplitude reflections, is located at a mean depth of 0.8 s (twt) below the seafloor, although locally the sedimentary cover above the igneous crust is absent. Five discontinuities characterized by high-amplitude continuous reflectors (named A–E, from top to bottom) separate six seismic units (named I–VI, from top to bottom) that are regionally identified across the area (Fig. 11; Table 2). The unit boundaries are conformable or slightly erosional above the underlying deposits and are overlain by discontinuous reflectors, which are either conformable or exhibit downlap terminations.

5.1. Seismic units

The depositional units show an irregular distribution due to the complex relief of the basement

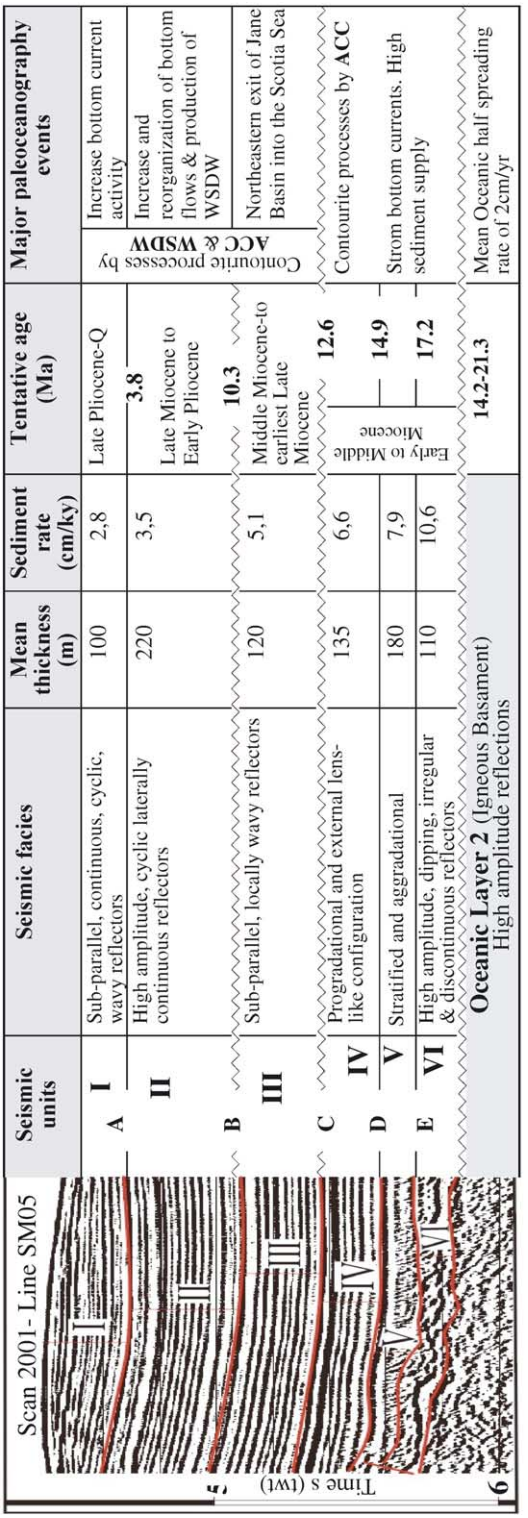

Fig. 11. Summary of the seismic stratigraphy of the depositional sequences above the igneous oceanic Layer 2 based on the MCS profiles. The main characteristic and tentative age of the six seismic units and reflectors identified in the area are summarized. See Fig. 13 and Table 2 for details on ages and sedimentation rates. Discussion in the text.

Table 2
Thickness, estimated sedimentation rates, the reflector (Reflector A–E) ages, and the age of the igneous basement Layer 2 (Fig. 12), of the depositional units (Units I–VI), calculated in three representative stratigraphic sections selected in MCS profile MC 03 (Fig. 10)

Units	Thickness (m)			Mean (m)
	Section 1	Section 2	Section 3	
I	108	104	98	103
II	206	221	236	221
III	147	97	118	121
IV	79	100	226	135
V	216	148	167	177
VI	49	135	147	110
Units	**Sedimentation rates (cm/ky)**			**Mean (cm/ky)**
	Section 1	Section 2	Section 3	
I	3.3	2.3	2.6	2.7
II	4.1	3.4	4.1	3.8
III	8.2	4.2	4.7	5.7
IV	3.6	5.0	5.5	4.7
V	10.8	6.2	6.7	7.9
VI	7.0	7.1	8.2	7.4
Reflectors	**Age range (Ma)**			**Mean (Ma)**
	Section 1	Section 2	Section 3	
A	3.2	4.6	3.7	3.8
B	8.2	11.0	9.5	9.6
C	10.0	13.3	12.0	11.8
D	12.2	15.3	16.1	14.5
E	14.2	17.7	18.6	16.8
Basement	14.9	19.6	20.4	

See Fig. 13.

and to thickness variations caused by depositional processes (Fig. 10). Basement highs locally crop out to produce a very rugged seafloor. The depositional units tend to be best developed over basement depressions and where large sediment drifts are formed due to the interference between basement topography and the bottom contour flows (Fig. 5 and 10).

Seismic Unit I corresponds to the youngest deposits identified in MCS profiles (Fig. 11). It is characterized by sub-parallel, gently undulating and wavy reflectors that show onlap and pinching out terminations over the lower boundary. A cyclic pattern of alternating low- and high-ampli-

tude internal reflectors is distinctly observed in the deposits. The seismic facies of the uppermost reflectors are best seen in the high resolution profiles described above. The thickest deposits correspond with the contourite drifts of the northern area (Figs. 9 and 10).

Seismic Unit II shows erosional truncation at the upper boundary. The internal seismic facies are constituted by sub-parallel, laterally continuous wavy reflectors, which become expansive over the area. These reflectors also have a cyclic pattern, but less marked than in Unit I. The internal reflectors show low-angle onlap and downlap terminations over an underlying high-amplitude, laterally continuous reflector B (Figs. 10 and 11). This reflector is locally erosional and it corresponds to a major discontinuity in the area. This discontinuity recorded the most important change in the style of deposition from the underlying depositional sequences, as shown by the expansive and aggradational character, and significant lateral continuity of the wavy reflectors of Unit II.

The top boundary of Seismic Unit III is also characterized by erosional truncation. This unit contains internal sub-parallel, locally wavy reflectors distinguished by a generalized northward oriented progradational pattern (Figs. 10 and 11). The reflectors have an onlap termination over the lower boundary. The thickness of the unit is controlled by the basement irregularities, pinching out against morphological highs and showing a general tendency to a northwards thinning. Reflector C at the base of Unit III is another major discontinuity over the area: it marks the change in the style and direction of progradation of the internal reflectors, which become northward oriented in the southern area above reflector C.

The upper boundary of Unit IV is characterized by a progradational pattern over the area. This unit has an external lens-like configuration influenced by the morphological highs of the igneous crust (Fig. 10). The internal reflectors are characterized by foresets. The progradation locally shows a distinct southwards trend, opposite to the orientation of the overlying units.

Seismic Unit V is composed of two packages (Figs. 10 and 11). The lower sub-unit shows an aggradational seismic pattern, with high-amplitude reflectors. It has a distribution that is restricted to the middle–southern region and pinches out towards a high of the basement. The upper package is characterized by well stratified internal reflectors, with aggradational configuration and a lens-like external shape. It is distributed throughout the area, with the exception of the northern region.

Seismic Unit VI fills in the basement (Figs. 10 and 11). The high-amplitude internal reflectors are highly dipping, irregular and laterally discontinuous. The distribution of this unit is uneven since it is observed only in basement depressions.

5.2. Age of the oceanic crust

The analysis of total field magnetic anomaly data provides the age of the crystalline basement of the oceanic crust. Because boreholes do not exist in this area, these determinations help to constrain the age of the depositional units that overlie the igneous crust. Previous studies in the northwestern sector of the surveyed region show short segments with linear magnetic anomalies corresponding to chron C5C and C6 that trend W–E (British Antarctic Survey, 1985). The age of the oceanic crust according to these anomalies is between 16.0 and 20.1 Ma, based on the timescale of Cande and Kent (1995). These anomalies indicate a N–S trend of extension and a younger northward oceanic crust.

The new data acquired during the SCAN2001 survey consisted of several long lines and a grid of short lines covering the northwestern sector of Discovery Bank (Fig. 1B). The most representative long profiles are located in the western side of the surveyed area and have a N–S trend, orthogonal to the linear magnetic anomalies. The identification of the same anomalies in parallel profiles helps to determine and confirm the E–W trend for the linear magnetic anomalies in this sector. In addition, there are local magnetic anomalies that are probably related to the recent volcanism recorded in the region.

We have modeled the magnetic data along seismic profile SM03 (Fig. 12). The MCS profile reveals that the top of the crystalline Layer 2 of the

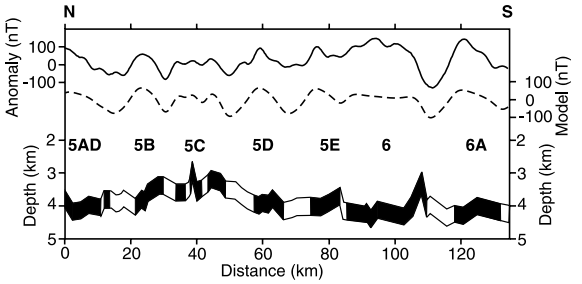

Fig. 12. Modeled magnetic anomaly for profile SM03 orthogonal to the magnetic anomaly trends. The timescale of Cande and Kent (1995) is used. An 0.5-km thick magnetized layer is assumed, the upper surface corresponds to a smoothed version of the observed top of Layer 2 of the oceanic crust. See Fig. 10 for the MCS profile SM03 and Fig. 3 for location of profile.

oceanic crust is overlain by a sedimentary cover of variable thickness. We assumed a thickness for the magnetized layer of 0.5 km and a mean magnetization of the oceanic crust of 2 A/m. The dipole field was used to determine the declination and inclination of the remnant magnetization, considering that the crust was formed approximately at the same latitude it occupies at present. Using the Cande and Kent (1995) geomagnetic polarity timescale, we modeled the profile and found a complete set of anomalies that range from chron C6A (20.9–21.3 Ma) to chron C5AD (14.2–14.6 Ma). The model was obtained with the Gravmag program (Pedley et al., 1993), and it shows a good fit between the calculated and observed anomalies (Fig. 12). The locations of our anomalies at chron C6 and chron 5C are, however, displaced in relation to those of British Antarctic Survey (1985), which may well result from navigation errors of the earlier magnetic profiles. The model provides a mean oceanic spreading rate of about 2 cm/yr for the southern flank of the spreading ridge, probably located north of the swath map area. Our data also confirm a N–S opening of this sector of the Scotia Plate.

On the basis of these data, the older sediments at the base of the depositional sequences would have ages ranging between Early Miocene (21.3 Ma) for the southern part and Middle Miocene (14.2 Ma) for the northern sector.

5.3. Age of the reflectors and depositional units

The age of the reflectors A–E was tentatively estimated for three representative stratigraphic sections selected on MCS profile MC03 (Figs. 10 and 13). The basic parameters used for the calculation are the age of the igneous basement derived from the modeled profile of the magnetic anomalies and the total thickness of the depositional sequence for each section (Figs. 10 and 12). The travel time depth (twt) of the reflectors was converted into depth in meters using the stacking velocity derived from the MCS profile velocity analysis and complemented with the results of refraction experiments in the nearby Powell Basin for the total depositional sequence (King et al., 1997).

In order to estimate the age of each reflector, we defined a sedimentation rate curve for each stratigraphic section (Fig. 13). This curve is constrained by: (1) the sedimentation rate of the nearby surface sediment cores, and (2) the results of the ODP boreholes on the Antarctic Peninsula and northern Weddell Sea. A core collected south of the swath map area, in the Scotia Sea, shows sedimentation rates of 3.3 cm/ky for the last 18 ky (Pudsey and Howe, 1998). ODP Site 1095 on a sediment drift setting of the Antarctic Peninsula Pacific margin also exhibits a low sedimentation rate for the Quaternary (2.5 cm/ky), which increases sharply for the underlying units of Pliocene (5–7 cm/ky) and Late Miocene (11 cm/ky) age (Barker et al., 1999). Sedimentation rates measured from ODP sites in the Jane Basin and Weddell Sea are also low for the Quaternary and Late Pliocene (less than 3 cm/ky) and increase downcore, except for the Middle–Late Miocene (1–2 cm/ky), reaching about 10 cm/ky in the early Middle Miocene (Barker et al., 1988).

The sedimentation rates obtained on the basis of the above calculations show some differences for each stratigraphic section, particularly for units III and V, but they are consistent for the other units (Table 2). These sedimentation rates were averaged over the area in order to obtain an estimated mean age of the reflectors and stratigraphic units. These mean sedimentation rates estimated in the swath area vary between about 2.7

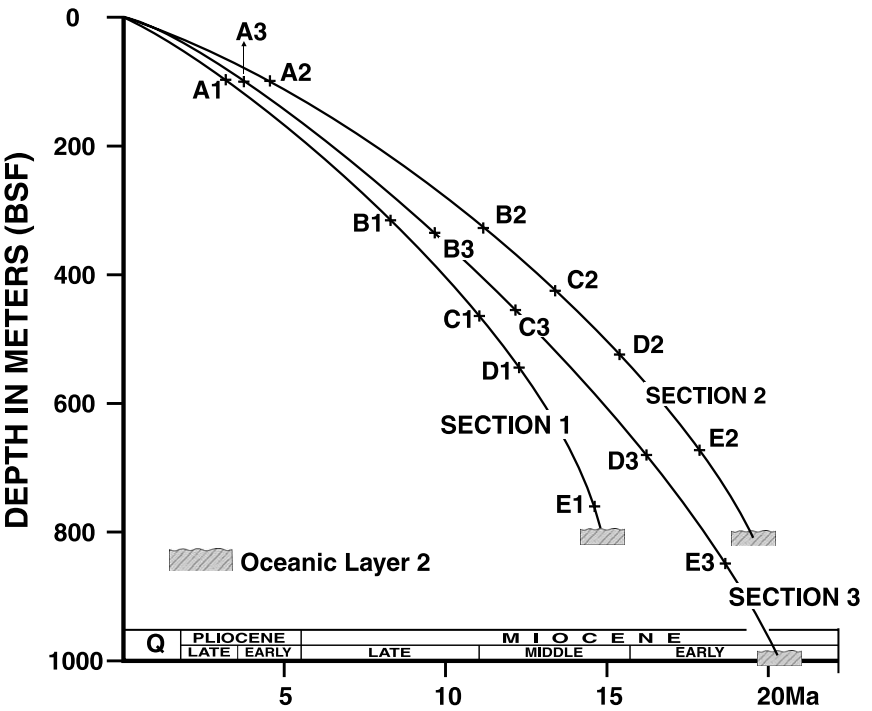

Fig. 13. Binary plots showing the relationships between the depth of the main reflectors below seafloor in the MCS profiles and the age of the crystalline basement of three representative locations. Sedimentation rate curves are tentatively extrapolated on the basis of the ODP borehole data from the Antarctic Peninsula and Weddell Sea areas and from gravity cores of the Scotia Sea for the Late Quaternary. See Fig. 10 for location of the three sections. Depth in meters below seafloor (BSF). Explanation in the text.

cm/ky for the uppermost unit and about 7.4–7.9 cm/ky for the lowermost deposits of Early Miocene age (Fig. 13; Table 2). A similar trend in sedimentation rates is well established around Antarctica (Barker et al., 1995).

5.4. Stratigraphic evolution

The contourite drift and sediment wave seismic facies of Seismic Unit I are about 100 m thick with a mean sedimentation rate of 2.7 cm/ky, according to our calculations and considering the uncertainties due to the absence of deep boreholes in the central Scotia Sea (Figs. 11 and 13; Table 2). Unit I has an estimated Late Pliocene–Quaternary age. It shows a marked cyclic sedimentation pattern, while the margins of the contourite drifts are affected by erosion, and it is less extensive than the underlying Unit II, (Fig. 10). The deposits of this unit were influenced by the contemporary and ancestral ACC and WSDW currents in the Scotia Sea. Unit II has a mean thickness of 220 m, with an average sedimentation rate of 3.8 cm/ky, and an estimated age of Late Miocene–Early Pliocene (Fig. 11; Table 2). The seismic facies of Unit II are similar to those of Unit I, although the deposits are more extensively distributed over the area (Fig. 10).

The mean thickness of Unit III is 120 m, with a sedimentation rate of 5.7 cm/ky. This unit, estimated to be of late Middle Miocene to earliest Late Miocene age, progrades northward in the southern area (Fig. 11; Table 2). The mean thickness of Unit IV is 135 m, with an estimated sedimentation rate of 4.7 cm/ky (Fig. 11; Table 2). The most diagnostic depositional feature of this

unit is a southward progradational pattern of the reflectors in the southern area, in contrast to the overlying units.

The mean thickness of Unit V is 180 m, with a sedimentation rate of 7.9 cm/ky, and an age estimated between the latest Early Miocene and the early Middle Miocene (Fig. 11; Table 2). This unit is aggradational and characterized by mounded, lens-like deposits of restricted distribution that are controlled by the basement topography. The mean thickness of Unit VI is 110 m, with a relatively high sedimentation rate estimated at 7.3 cm/ky. Unit VI is of Early Miocene age and it overlies the igneous basement (Fig. 11; Table 2). The progradational character and steep reflectors of this unit are indicative of a high energy environment and a relatively large sediment supply.

6. Discussion: the ACC and the WSDW flows

6.1. Contourite deposits in the central Scotia Sea

Contourite deposits were previously described on the basis of 3.5-kHz records and sediment cores in the Scotia Sea (Pudsey and Howe, 1998). These authors identified several types of echo character and show the importance of contourite sheet and mounded contourite drifts during the Quaternary. They reported, however, an absence of contourite sediment waves in the area, which they interpreted as the result of the unsteadiness of the ACC flow. Our seismic profiles exhibit, in contrast, a more complete set of contourite deposits that include abundant contourite sediment waves. The swath bathymetry from the multibeam sonar shows the extensive surface distribution of these contourite deposits, which cover most of the swath map area except for areas of erosion and non-deposition due to strong bottom flows (Figs. 3–5). In this respect, current meter moorings in the central Scotia Sea, 50 m above the seabed, recorded short periods of high velocity currents of up to 50 cm/s (Pudsey and Howe, in press).

Contourite deposits are well illustrated in several Antarctic continental margin areas. Large sediment drifts occupy a significant part of the continental rise of the Pacific margin of the Antarctic Peninsula (Rebesco et al., 1997). The sediment drifts seem to be constructed from the fine-grained components of turbidity currents, which are entrained and transported southwest by bottom currents (Rebesco et al., 1996; Camerlenghi et al., 1997). A similar model is proposed for high relief mounded contourite-style deposits developed in the Wilkes Land continental rise (Escutia et al., in press). The influence of the WSDW flows from the Weddell Gyre is also recognized in the depositional patterns of an extensive sediment wave field covering an area of over 1000 km^2 on the continental rise of the Powell Basin (Howe et al., 1998). Many of these contourite deposits seem to result from downslope turbidite flows entrained by nepheloid layers within the ambient, weak bottom currents. In the Scotia Sea, our swath bathymetry map and seismic profiles exhibit, in contrast, contourite deposits and erosional features indicative of high energy bottom current flows, that occasionally are intensified when channelized along narrow paths, whereas the rest of the seabottom is affected by less energetic currents (Figs. 2 and 14).

The occurrence of contourite drifts is largely influenced by the seafloor relief. Elongate-mounded drifts tend to develop particularly in areas adjacent to intensified bottom flows, which are concentrated along channels or narrow constrictions (Figs. 3 and 4). The deposits become banked against the bottom prominences away from the most energetic currents, as the result of the differential settling and escape of the fine-grained particles from the main flows (Nelson et al., 1993; Faugeres et al., 1999). The orientations of the axes of these thick-mounded deposits reflect the flow distribution of the ACC and WSDW in the central Scotia Sea (Fig. 14B). The flows are initially diverted around the primary relief of the basement, which enhanced flow concentration along the depressions and favored the differential deposition on the topographic highs, away from the main flow. Once the drift deposition began, the successive flows were concentrated around the primary deposits, promoting growth along the axis of the drift, whereas only thin deposits and erosion occur at the drift margins and channels

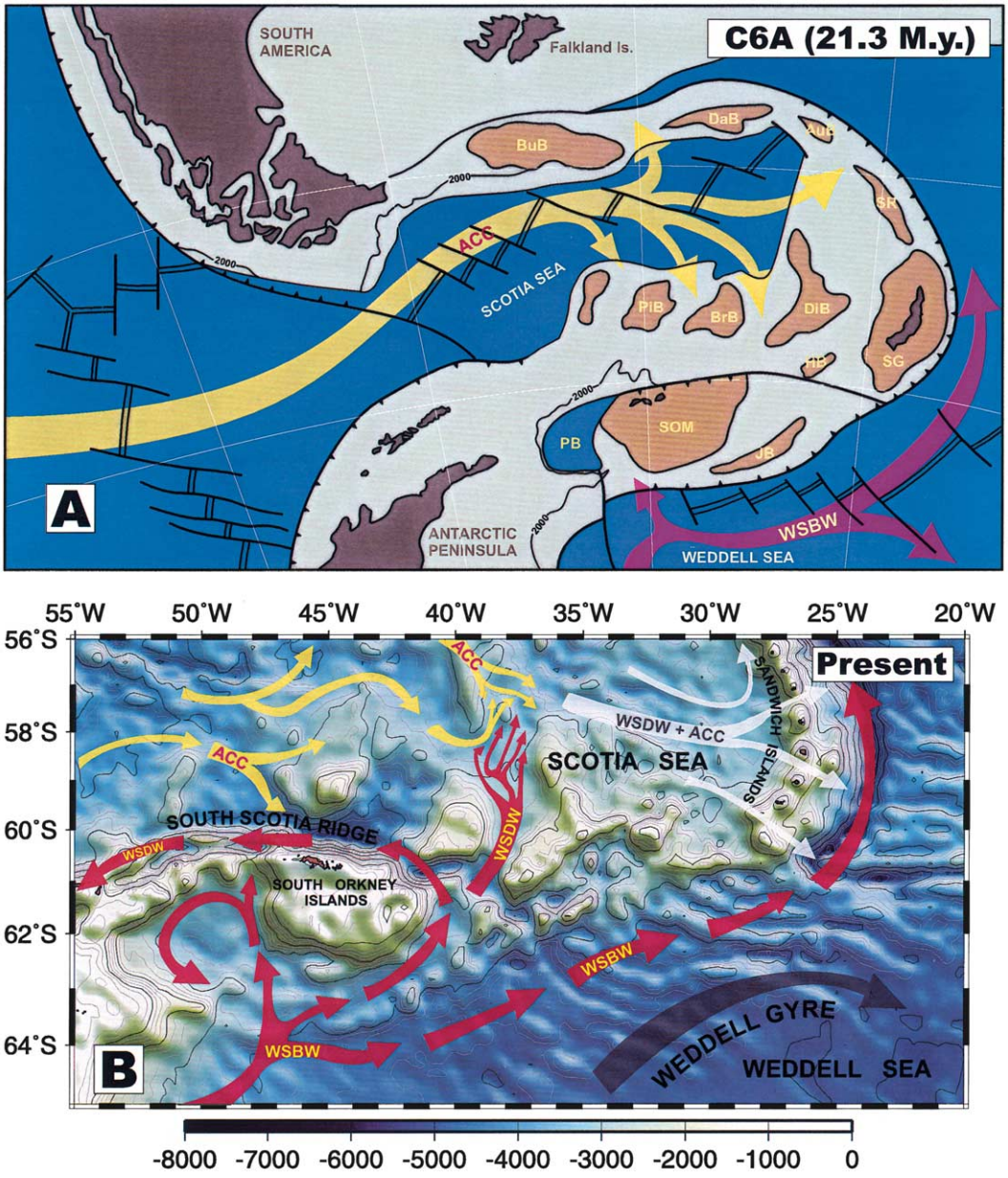

Fig. 14. (A) Interpretative tectonic sketch of the Scotia Sea and location of continental blocks at chron C6A (21.3 Ma) showing the bottom water flow patterns. Legend: AuB, Aurora Bank; BrB, Bruce Bank; BuB, Burdwood Bank; DaB, Davis Bank; DiB, Discovery Bank; HB, Herdman Bank; JB, Jane Bank; PB, Powell Basin; PiB, Pirie Bank; SG, South Georgia; SR; Shag Rocks; SOM, South Orkney Microcontinent. (B) Sketch of bottom water flows in the northern Weddell Sea and the eastern Scotia Sea, showing the possible ways of deep water of the ACC and the WSDW/WSBW related Weddell Sea Gyre. The interaction between these two flows in the central Scotia Sea develops a large variety of contourite deposits. See text for the tectonic reconstruction and bottom water flow discussion.

(Fig. 5). In addition, the elongate-mounded drifts appear to be more extensively developed along the left (downstream) margins of major channelized flows; i.e. drift W2, left margin of WWC; drifts A3, left margin of SAC; drift A1, left margin of MAC (Fig. 5; Table 1). We propose that this preferential sediment deposition is related to the influence of the Coriolis force on the flows, which are diverted westward from the main channelized currents.

A contourite fan occupies the central area of the swath map (Fig. 5). The fan is characterized by a main feeder channel located at the exit of the Jane Basin from the northern Weddell Sea, which follows the base-of-slope of a large submarine bank (Fig. 14B). The channel coincides with the northward path of the WSDW, which is constrained in a gap through the South Scotia Ridge. The fan develops downstream from the mouth of a main feeder channel, which splits into two distributaries and develops a subdued proximal fan morphology intersected by sediment waves and, in the middle and distal part, is incised by furrows (Fig. 8). The development of the contourite fan is favored by the morphology of the sea-bottom that allows the overbank flows of the two main distributary channels to span over a wide, gentle sloping surface and to develop aggradational deposits. The swath map area we studied is isolated from any direct continental sediment supply; consequently, the source of sediments to form these deposits must be the WSDW, the flow of which is concentrated at the exit of the Jane Basin into the Scotia Sea and is probably enriched in ice-rafted sediments below the frontal edge of the sea ice.

Two sets of sediment waves are observed and also reflect flow distribution patterns. Large sediment waves are best developed in the area of confluence between the ACC and WSDW flows (Fig. 5). The sediment waves migrate southeastward in the northern area under the influence of the ACC, whereas those of the southern sector show a predominantly northern trend as a result of the influence of the WSDW. Small sediment waves are best developed in areas influenced only by a predominant flow direction. Their development is controlled by the presence of basement relief and obstacles that intersect the flow path.

6.2. Seaways and paleoceanographic implications

The initiation of the ACC following the opening of the Drake Passage is generally considered the most important event controlling the evolution of the Cenozoic climate and one of the crucial factors that influenced the development of the extensive Antarctic ice sheets during the Miocene (Kennett, 1977; Barrett, 1996; Pudsey and Howe, 1998). It is also well known that the Scotia Sea region was the location for the final barrier to a complete circum-Antarctic deep-water flow, although its consequences and the significance of its effect for the evolution of global climate is not yet well established (Lawver et al., 1992; Barrett, 1996; Barker, 2001). A major change of the water temperature in the southern oceans occurred during the earliest Oligocene, which seems to be related to the opening of the deepwater seaways (Kennett and Stott, 1990; Mead et al., 1993). More recently, however, it has been questioned whether a deep circumpolar passageway alone is sufficient to produce a strong current and the subsequent permanent ice sheets of the East Antarctic (Lawver and Gahagan, 1998). The opening of the Drake Passage and a passage south of Australia are necessary for the development of the ACC. However, the closure of mid-latitude and equatorial seaways, including the Tethys ocean in the Early Cenozoic, Southeast Asia with Australia in Miocene, and finally the Isthmus of Panama in Pliocene times (Coates et al., 1992), are proposed to block and divert the westward flows of equatorial waters, producing a major change in the ocean water temperatures and causing a gradual cooling (Lawver and Gahagan, 1998). For example, the closure of the Panama passageway between South and North America during the Pliocene forced formation of dense, warm surface water with a higher evaporation rate in the North Atlantic which led to a greater evaporation and the production of more saline deep water in the North Atlantic (Warren, 1983; Coates et al., 1992; Droxler et al., 1998). The higher production of dense North Atlantic Deep Water is proposed to have had a significant effect on climate and, consequently, have influenced the Pliocene development of massive polar ice sheets. We propose

that in addition to the development of a strong ACC, the opening of seaways in the Drake Passage led to the production of AABW that later flowed into the South Atlantic. Though there is no evidence of WSDW in the Scotia Sea prior to the development of the deep seaways, we suggest that WSBW was already forming outside the Scotia Sea and exiting into the Southern Atlantic around the Scotia Arc (Fig. 14A). This flow, in addition, was probably intensified as a result of the creation of deep seaways into the Scotia Sea, which led to significant paleoceanographic changes during the Early Miocene. The ages of the oceanic crust show that before chron C6A (20.7 Ma) none of the central and eastern Scotia Sea existed (British Antarctic Survey, 1985). The western Scotia Sea and Drake Passage were smaller (Maldonado et al., 1994, 2000). The Shackleton Fracture Zone across the Drake Passage was experiencing extensional tectonic deformation and most probably had a relief less important than that of today, at least in the segments away from spreading centers (Maldonado et al., 2000; Galindo-Zaldívar et al., 2001). Most of the present relief of this fracture zone was developed by a thickened oceanic crust formed shortly after anomaly C3A (6 Ma), when spreading ceased in the West Scotia Ridge (Fig. 14A). The South Scotia Ridge was less fragmented and a more consistent barrier during the Early Miocene (King et al., 1997; Maldonado et al., 1998). The Discovery, Bruce and Pirie banks probably formed a continuous continental fragment close to the South Orkney Microcontinent, which blocked the SE Scotia Sea (Fig. 14A). These banks, bounding small internal basins, probably opened later, as in the case of the Protector Basin which developed during the Middle–Late Miocene (Galindo-Zaldívar et al., 2001). The northeastern exit of the Jane Basin into the Scotia Sea was also probably closed by the continental fragments, since an east–west strike-slip fault offset the banks along the northern margin of the South Scotia Ridge during the different phases of the tectonic evolution (Galindo-Zaldívar et al., 1996, 2001; Maldonado et al., 1998).

The proposed reconstruction has several important paleoceanographic implications (Fig. 14A). First, the Scotia Arc formed a smaller barrier to deep water outflow, although the Drake Passage was a well developed seaway for deep water circulation at chron C6A (21.3 Ma). Thus, a strong outflow may have been inhibited by the North Scotia Ridge and the ACC could not have developed if the North Scotia Ridge was a continuous elevated barrier (Barker, 2001). Second, bottom waters from the Weddell Gyre were diverted eastwards and also northeastwards around the Scotia Arc and as a consequence inhibited from entrance into the Scotia Sea (Fig. 13A). Under these circumstances, a significant ACC deep water flow would not have existed in the Scotia Sea during the Early Miocene. Our MCS profiles show, in contrast, that deep water circulation was active in the central Scotia Sea since the earlier stages of opening of this segment of seafloor (Fig. 10). All the depositional units exhibit discontinuous internal reflectors, frequently characterized by wavy configuration patterns. Towards the base of the units oblique and sigmoid configuration patterns are observed, which downlap the reflector boundary. The overall seismic character indicates energetic bottom currents, which developed contourite drift and sediment wave deposits with high sedimentation rates during the Early Miocene. Increased sediment supply was provided during the early stages of the opening of the Drake Passage and western Scotia Sea by the continental fragments now dispersed around the Scotia Arc, in addition to the South American and Antarctic Peninsula margins (Fig. 14A). The deposits exhibit, however, several differential characteristics, which indicate an evolution in the nature of the bottom flows, sediment supply and bottom current distribution. The older depositional units VI and V above the crust recorded strong bottom current flows and high sediment supply, which infilled depressions. The units have a wedge, mounded geometry and wavy reflectors all indicative of active flows. The internal reflectors of Unit IV (Middle Miocene) show a southward migration pattern, which is attributed to the influence of an active ACC flow into the central Scotia Sea in that direction. During these earlier stages in the development of the Scotia Sea the bottom part of the ACC flow entering into the

Scotia Sea was forced into a clockwise gyre due to Coriolis and developed the important southward prograding sediment drifts (Fig. 14A). The initial incursions of the WSDW into the Scotia Sea are observed in the deposits of Unit III, during the Middle Miocene, which record a northward progradational pattern similar to the uppermost deposits (Figs. 10 and 11). This evolution in the depositional sequences and bottom processes was controlled by the opening of gaps in the South Scotia Ridge and the connection of the Weddell Sea and Scotia Sea through the Jane Basin (Fig. 14). Another important aspect of the opening of deep seaways is the westward escape of part of the WSDW through gates of the South Scotia Ridge towards the Pacific. This water mass is responsible at present, and probably was in the past, for the southwest contour flow that partly controlled the growth of the sediment drifts of the Pacific margin of the Antarctic Peninsula (Camerlenghi et al., 1997). According to the seismic interpretation of Rebesco et al. (1997), the drift growth stage started in the Middle Miocene, which coincides with the age of deepening of the gateways and first incursions of the WSDW in the Scotia Sea proposed in this paper.

Units I and II are characterized by a distinct cyclic pattern of deposition, more continuous wavy deposits and the development of internal unconformities, all of which attest to increased bottom current energy and intensified bottom current activity. The two units record a change in the style of deposition and the environmental parameters over the area. The estimated time for reflector B at the base of Unit II is early Late Miocene (Fig. 11; Table 2) and this unconformity may date the reorganization of bottom flows and the production of WSDW. The deposit at ODP Site 1095 began to develop a distinct cyclic pattern at about 9 Ma (Barker et al., 1999). The evolution in the depositional style at Site 1095 was attributed to the initiation of glacial cycles in the Antarctic Peninsula margin and the influence of advancing–retreating, grounded ice sheets over the shelf, which controlled sediment supply and depositional processes. The discontinuity between Unit I and II, reflector A, is interpreted to be of Late Pliocene age (Fig. 11; Table 2). This reflector records an increase in bottom current activity as indicated by the development of extensive erosional surfaces. The increased current activity may reflect an intensified deep water production and predate the onset of the Northern Hemisphere continental glaciations and massive Antarctic ice sheets during the Late Pliocene.

7. Conclusions

The swath map and seismic profiles of the central Scotia Sea exhibit contourite morphologies and seismic facies including a contourite fan and several types of sediment drift and wave deposits (Fig. 5). The contourite deposits cover the surface of the investigated area, except where the igneous basement crops out at the seafloor due to intense bottom currents. These deposits are also well developed throughout the stratigraphic sequence above the igneous oceanic crust of Early Miocene age (Fig. 11). The extensive distribution and the predominance of contourite deposits verify the importance of deep water flows in the Scotia Sea. The deposits result from an interplay between the northward flowing WSDW and the eastward directed flow of the ACC, which are influenced by the Coriolis force. Major evolutionary changes in the seismic facies, however, indicate that the environmental parameters and bottom current distribution patterns varied over time (Fig. 11).

The older deposits above the igneous oceanic crust of Early–Middle Miocene age (chron C5AD to C6A) exhibit a rapid progradational pattern and relatively high sedimentation rates (Fig. 10 and 11; Table 2). These deposits were developed by a strong, southward oriented flow of the ACC in the central Scotia Sea, whereas the WSBW flows were diverted around the Scotia Arc due to the morphologic barrier imposed by the South Scotia Ridge (Fig. 14A). The first evidence for northward oriented WSDW flows in the central Scotia Sea is observed in Unit III, during the Middle Miocene (Fig. 11). A major unconformity below Unit II and a change in the depositional seismic facies may predate the onset of major grounding of ice sheets on the Antarctic

Peninsula shelf. The deposits above this unconformity record intensified bottom currents and probably a significant decrease in sedimentation rates. Unit II is expansive over the area and exhibits an extensive development of contourite deposits. The unconformity below Unit I, of Late Pliocene–Quaternary age, also predates an intensification of bottom currents and probably the onset of the major continental polar glaciations and major Antarctic ice sheets.

Acknowledgements

We thank the Commander, officers and crew of the B/O *Hespérides* for their support in obtaining the data presented in this paper under sometimes severe sea conditions. The diligence and expertise of engineers E. Litcheva and J. Maldonado who processed the MCS data and swath bathymetry is appreciated. We are indebted to Dr. Anatoli Schreider for his instrumental help in processing the magnetic anomaly profiles. We thank J. Rodero, M.J. Román and A. Caballero for their help in preparing the figures and the electronic version of this paper. Drs. C. Hans Nelson and Carlota Escutia provided helpful reviews that improved the original version of the manuscript. We are also indebted to referees Drs. Angelo Camerlenghi and John A. Howe for their final review of the paper and comments. The results of this work are related to IGCP-432 project Contourites, Bottom Currents and Palaleocirculations. The Spanish Comisión Interministerial de Ciencia y Tecnología (CYCIT) supported this research through Projects ANT99-0817 and REN2001-2143/ANT.

References

Barker, P.F., 1995. The proximal marine sediment record of Antarctic climate since the Late Miocene. In: Cooper, A.K., Barker, P.F., Brancolini G. (Eds.), Geology and Seismic Stratigraphy of the Antarctic Margin. AGU Antarctic Research Series 68, pp. 25–57.

Barker, P.F., 2001. Scotia Sea regional tectonics evolution: Implications for mantle flow and palaeocirculation. Earth-Sci. Rev. 55, 1–39.

Barker, P.F., Burrell, J., 1977. The opening of Drake Passage. Mar. Geol. 25, 15–34.

Barker, P.F., Dalziel, I.W.D., Storey, B.C., 1991. Tectonic development of the Scotia Arc region. In: Tingey, R.J. (Ed.), The Geology of Antarctica. Oxford University Press, Oxford, pp. 215–248.

Barker, P.F., Kennett, J.P., O'Connell, S.B., et al., 1988. Proc. ODP, Init. Repts. 113. Ocean Drilling Program, College Station, TX, 785 pp.

Barker, P.F., Camerlenghi, A., Acton, G.D., et al., 1999. Proc. ODP, Init. Repts. 178 (CD-ROM). Available from: Ocean Drilling Program, Texas A&M University, College Station, TX 77845-9547 (CD-ROM volume 1096–2522).

Barrett, P.J., 1996. Antarctic palaeoenvironment through Cenozoic times – A review. Terra Antarct. 3, 103–119.

British Antarctic Survey, 1985. Tectonic Map of Scotia Arc, Sheet (Misc.) 3, Scale 1:3,000,000. British Antarctic Survey, Cambridge.

Camerlenghi, A., Crise, A., Pudsey, C.J., Accerboni, E., Laterza, R., Rebesco, M., 1997. Ten month observation of the bottom current regime across a sediment drift of the Pacific margin of the Antarctic Peninsula. Antarct. Sci. 9, 424–431.

Cande, S.C., Kent, D.L., 1995. Revised calibration of the geomagnetic polarity timescale for the Late Cretaceous and Cenozoic. J. Geophys. Res. 100, 6093–6095.

Coates, A.G., Jackson, J.B.C., Collins, L.S., Cronin, T.M., Dowsett, H.J., Bybell, L.M., Jung, P., Obando, J.A., 1992. Closure of the Isthmus of Panama: The near-shore marine record of Costa Rica and western Panama. Geol. Soc. Am. Bull. 104, 814–829.

Diester Haass, L., Zahn, R., 1996. Eocene–Oligocene transition in the Southern Ocean: History of water mass circulation and biological productivity. Geology 24, 163–166.

Droxler, A.W., Burke, K.C., Cunningham, A.D., Hine, A.C., Rosencrantz, E., Duncan, D.S., Hallock, P., Robinson, E., 1998. Caribbean constraints on circulation between Atlantic and Pacific Oceans over the past 40 million years. In: Crowley, T.J., Burke, K.C. (Eds.), Tectonic Boundary Conditions for Climate Reconstructions. Oxford University Press, Oxford, pp. 169–187.

Duplessy, J.C., Shackleton, N.J., Fairbanks, R.G., Labeyrie, L.D., Oppo, D., Kallel, N., 1988. Deep water source variations during the last climatic cycle and their impact on the global deep water circulation. Paleoceanography 3, 343–360.

Escutia, C., Nelson, C.H., Acton, G.D., Cooper, A.K., Eittreim, S.L., Warnke, D.A., Jaramillo, J., in press. Current controlled deposition on the Wilkes Land continental rise. In: Stow, D.A.W., Pudsey, C.J., Howe, J.A., Fauguères, J.C. (Eds.), Atlas of Deep-Water Contourite Systems. Mem. Geol. Soc. Lond. (in press).

Fahrbach, E., Rohardt, G., Schröder, M., Strass, V., 1994. Transport and structure of the Weddell Gyre. Ann. Geophys. 12, 840–855.

Faugeres, J.C., Stow, D.A.V., Imbert, P., Viana, A., 1999. Seismic features diagnostic of contourite drifts. Mar. Geol. 162, 1–38.

Foldvik, A., Gammelrsød, T., 1988. Notes on Southern Ocean hydrography, sea-ice and bottom water formation. Palaeogeogr. Palaeoclimatol. Palaeoecol. 67, 3–17.

Foster, T.D., Middleton, J.H., 1979. Variability in the bottom water of the Weddel Sea. Deep-Sea Res. 26, 743–762.

Foster, T.D., Middleton, J.H., 1980. Bottom water formation in the western Weddell Sea. Deep-Sea Res. 27, 367–381.

Galindo-Zaldívar, J., Jabaloy, A., Maldonado, A., Sanz de Galdeano, C., 1996. Continental fragmentation along the South Scotia Ridge transcurrent plate boundary NE Antarctic Peninsula. Tectonophysics 242, 275–301.

Galindo-Zaldívar, J., Maldonado, A., Barnolas, A., Bohoyo, F., Hernández-Molina, J., Gamboa, L., Pereira, A.J., Rodríguez-Fernández, J., Somoza, L., Suriñach, E., George, A. U., Vázquez, J.T., 2001. Continental crust fragmentation, small basin development and deep water circulation in the southern Scotia Sea (Southern Atlantic). In: Fernandes J., Lima de Lima, O. (Eds.), Seventh International Congress of the Brazilian Geophysical Society, Salvador, pp. 1555–1557.

Georgi, D.T., 1981. Circulation of bottom waters in the southwestern South Atlantic. Deep-Sea Res. 28, 959–979.

Gille, S.T., 1994. Mean sea-surface height of the Antarctic Circumpolar Current from Geosat data – Method and application. J. Geophys. Res. 99, 18255–18273.

Howe, J.A., Pudsey, C.J., 1999. Antarctic Circumpolar Deep Water: A Quaternary paleoflow record from the northern Scotia Sea, South Atlantic Ocean. J. Sediment. Res. 69, 847–861.

Howe, J.A., Livermore, R.A., Maldonado, A., 1998. Mudwave activity and current-controlled sedimentation in the Powell Basin, northern Weddell Sea, Antarctica. Mar. Geol. 149, 229–241.

IAGA, 2000. IAGA Division V, Working Group 8, International Geomagnetic Field – Epoch 2000, Revision of the IGRF for 2000–2005.

Kennett, J.P., 1977. Cenozoic evolution of Antarctic glaciation, the Circum-Antarctic Ocean, and their impact on global paleoceanography. J. Geophys. Res. 82, 3843–3859.

Kennett, J.P., Stott, L.D., 1990. Proteus and Proto-oceanus: Ancestral Paleogene oceans as revealed from Antarctic stable isotope results. In: Barker, P.F., Kennett, J.P., et al. (Eds.), Proc. ODP, Sci. Results 113. Ocean Drilling Program, College Station, TX, pp. 865–880.

King, E.C., Leitchenkov, G., Galindo-Zaldivar, J., Maldonado, A., Lodolo, E., 1997. Crustal structure and sedimentation in Powell Basin. In: Barker, P., Cooper, F. (Eds.), Geology and Seismic Stratigraphy of the Antarctic Margin, Part 2. AGU Antarctic Research Series 71, pp. 75–93.

Larter, R.D., King, E.C., Leat, P.T., Reading, A.M., Smellie, J.L., Smythe, D.K., 1998. South Sandwich slices reveal much about arc structure, geodynamics and composition. EOS Transactions, American Geophysical Union, 79, pp. 281, 284–285.

Lawver, L.A., Gahagan, L.M., 1998. Opening of Drake Passage and its impact on Cenozoic ocean circulation. In: Crowley, T.J., Burke, K.C. (Eds.), Tectonic Boundary Conditions for Climate Reconstructions. Oxford University Press, Oxford, pp. 212–223.

Lawver, L.A., Gahagan, L.M., Coffin, M.F., 1992. The development of paleoseaways around Antarctica. In: Kennett, J.P., Warnke, D.A. (Eds.), The Antarctic Paleoenvironment: A Perspective on Global Change, vol. 56. AGU Antarctic Research Series, pp. 7–30.

Livermore, R., McAddo, D., Marks, K., 1994. Scotia Sea tectonics from high-resolution satellite gravity. Earth Planet. Sci. Lett. 123, 255–268.

Locarnini, R.A., Whitworth, T., III, Nowlin, W.D.J., 1993. The importance of the Scotia Sea on the outflow of Weddell Sea Deep Water. J. Mar. Res. 51, 135–153.

Maldonado, A., Larter, R., Aldaya, F., 1994. Forearc tectonic evolution of the South Shetland margin, Antarctic Peninsula. Tectonics 13, 1345–1370.

Maldonado, A., Zitellini, N., Leitchenkov, G., Balanyá, J.C., Coren, F., Galindo-Zaldívar, J., Lodolo, E., Jabaloy, A., Zanolla, C., Rodríguez-Fernández, J., Vinnikovskaya, O., 1998. Small ocean basin development along the Scotia–Antarctica plate boundary and in the northern Weddell Sea. Tectonophysics 296, 371–402.

Maldonado, A., Balanyá, J.C., Barnolas, A., Galindo-Zaldívar, J., Hernández, J., Jabaloy, A., Livermore, R.A., Martínez, J.M., Rodríguez-Fernández, J., Sanz de Galdeano, C., Somoza, L., Suriñach, E., Viseras, C., 2000. Tectonics of an extinct ridge-transform intersection, Drake Passage (Antarctica). Mar. Geophys. Res. 21, 43–68.

McCave, I.N., Tucholke, B.E., 1986. Deep current controlled sedimentation in the western North Atlantic. In: Vogt, P.R., Tucholke, B.E. (Eds.), The Geology of North America, vol. M, The Western North Atlantic region, Decade of North America Geology. Geol. Soc. Am., Boulder, CO, pp. 451–468.

Mead, G.A., Hodell, D.A., Ciesielski, P.F., 1993. Late Eocene to Oligocene vertical oxygen isotopic gradients in the South Atlantic: Implications for Warm Saline Deep Water. In: Kennett, J.P., Warnke, D.A. (Eds.), The Antarctic Paleoenvironment: A Perspective on Global Change. AGU Antarctic Research Series, pp. 27–48.

Moore, J.K., Abbott, M.R., Richman, J.G., 1997. Variability in the location of the Antarctic Polar Front (90°–20°W) from satellite sea surface temperature data. J. Geophys. Res. 102, 27825–27833.

Nelson, C.H., Baraza, J., Maldonado, A., 1993. Mediterranean undercurrent sandy contourites, Gulf of Cadiz, Spain. Sediment. Geol. 82, 103–131.

Nowlin, W.D., Klinck, J.M., 1986. The physics of the Antarctic Circumpolar Current. Rev. Geophys. 24, 469–491.

Nowlin, W.D., Zenk, W., 1988. Westward bottom currents along the margin of the South Shetland island arc. Deep-Sea Res. 35, 269–301.

Orsi, A.H., Whitworh, T., III, Nowlin, W.D., Jr., 1995. On the meridional extent and fronts of the Antarctic Circumpolar Current. Deep-Sea Res. 42, 641–673.

Pedley, R.C., Bubsby, J.P., Dabek, Z.K., 1993. Gravmag v. 1.5. British Geological Survey.

Pelayo, A.M., Wiens, D.A., 1989. Seismotectonics and relative plate motions in the Scotia Sea region. J. Geophys. Res. 94, 7293–7320.

Peterson, R.G., Whitworth, T., III, 1989. The Subantarctic and Polar Fronts in relation to deep water masses through the Southwestern Atlantic. J. Geophys. Res. 94, 10817–10838.

Pudsey, C.J., 1992. Late Quaternary Changes in Antarctic Bottom Water velocity inferred from sediment grain size in the northern Weddell Sea. Mar. Geol. 107, 9–33.

Pudsey, C.J., Howe, J.A., 1998. Quaternary history of the Antarctic Circumpolar Current: Evidence from the Scotia Sea. Mar. Geol. 148, 83–112.

Pudsey, C.J., Murray, J.W., Ciesielski, P.F., 1987. Late Pliocene to Quaternary sedimentation on the South Orkney Shelf. Br. Antarct. Surv. Bull. 77, 81–97.

Pudsey, C.W., Howe, J.A., in press. Case study 27: Mixed biosiliceous–terrigenous sedimentation under the Antarctic Circumpolar Current, Scotia Sea. In: Stow, D.A.W., Pudsey, C.J., Howe J.A., Fauguères, J.C. (Eds.), Atlas of Deep-Water Contourite Systems. Mem. Geol. Soc. Lond. (in press).

Rack, F.R., 1993. A geologic perspective on the Miocene evolution of the Antarctic Circumpolar Current system. Tectonophysics 222, 397–415.

Rebesco, M., Larter, R.D., Camerlenghi, A., Barker, P.F., 1996. Giant sediment drifts on the continental rise west of the Antarctic Peninsula. Geo-Mar. Lett. 16, 65–75.

Rebesco, M., Larter, R.D., Barker, P.F., Camerlenghi, A., Vanneste, L.E., 1997. The history of sedimentation on the continental rise west of the Antarctic Peninsula. In: Barker, P.F., Cooper, A.K. (Eds.), Geology and Seismic Stratigraphy of the Antarctic Margin, part 2, vol. 71. American Geophysical Union, pp. 29–49.

Schröder, M., Fahrbach, E., 1999. On the structure and transport of the eastern Weddell Gyre. Deep-Sea Res. II 46, 501–527.

Warren, B.A., 1983. Why is no deep water formed in the North Pacific? J. Mar. Res. 41, 327–347.

Zenk, W.O., 1981. Detection of overflow events in the Shag Rocks Passage, Scotia Ridge. Science 213, 1113–1114.